View metadata, citation and similar papers at core.ac.uk

brought to you by CORE

provided by Elsevier - Publisher Connector

International Journal of Solids and Structures 46 (2009) 3902–3913

Contents lists available at ScienceDirect

International Journal of Solids and Structures

journal homepage: www.elsevier.com/locate/ijsolstr

Homogenization of a pressurized tube made of elastoplastic materials with discontinuous properties

George Chatzigeorgiou [a], Nicolas Charalambakis [a,*], Francois Murat [b]

[a] Institute of Mechanics of Materials, Division of Structures, Department of Civil Engineering, Aristotle University of Thessaloniki, GR 541 24, Greece
[b] Laboratoire Jacques-Louis Lions, Université Pierre et Marie Curie, Boîte courrier 187, 75252 Paris Cedex 05, France

ARTICLE INFO

Article history:
Received 24 May 2008
Received in revised form 21 July 2009
Available online 28 July 2009

Keywords:
Multilayered pressurized tube
Homogenization
Dissimilar elastoplastic materials
Induced anisotropy

ABSTRACT

In this paper we present the homogenization of a periodic multilayered pressurized tube made of very dissimilar elastoplastic materials. We focus on some aspects of technological importance, such as the effective properties, the behavior of the homogenized displacements and stresses, the discontinuities of hoop and longitudinal stresses, the homogenization-induced anisotropy. We conclude that the problem needs to be reformulated in order to be stable by homogenization and we define the effective elastic and incremental stress corrector matrices for the incremental stress–total strain matrix law. Finally, we present the numerical simulation for both the non-homogeneous and the homogenized material and two numerical examples confirming the theoretical results.

© 2009 Elsevier Ltd. All rights reserved.

1. Introduction

Efficient homogenization techniques are used to describe the overall behavior of highly heterogeneous materials, assumed to exhibit some simplistic properties, such as isotropy, smooth or continuous gradation of material properties, etc. Engineers some times rely on continuum theories that describe the effect of heterogeneities at a larger scale and in a more or less arbitrary "average" sense. In many cases such computations would deliver more information than it is required at a sufficiently low cost.

However, many homogenization procedures cannot guarantee that the effective characterization follows the characterization of the phases. Then it could be interesting to look for the conditions under which a given multiphase model is stable by homogenization. On the other hand, some effective descriptions of highly heterogeneous materials fail to capture the influence of the spatial scale of the heterogeneity on the overall response of the material. Mathematical homogenization provides a consistent definition of both the homogenized procedure and the homogenized equations. It consists in setting the problem as a sequence of equations describing the heterogeneous material when the heterogeneities, whose typical size is characterized by a parameter ε, become smaller and smaller. In periodic materials, the parameter ε defines the periodic microstructural scale relative to the entire body. For instance, in layered materials it may characterize the order of the thickness of the numerous thin layers. Then all field quantities ϕ^{ε} can be described in terms of two spatial scales, namely x and $y = x/\varepsilon$, where $\phi^{\varepsilon} = \phi(x,y) = \phi(x,x/\varepsilon)$. In linear elasticity problems, a multiscale field variable (asymptotic expansion) and the flow rule for the gradient operator $(\partial/\partial x_i + \frac{1}{\varepsilon}\partial/\partial x_i)$ can be used to separate the partial differential equations into equations of different scale orders leading to homogenized equations and effective parameters (Bakhalov and Panasenko, 1989). In nonlinear problems, the asymptotic homogenization is not generally applicable. Then, nonlinear functional analysis techniques should be used to prove that the mathematical problem is well posed, or at least that we are able to prove the existence of, at least, one solution of the problem and an *a priori* estimate for it in some functional space. The problem is then to try to pass to the limit when $\varepsilon \to 0$. This is a difficult task, since weak topologies are involved and since passing to the limit is a nonlinear process (even if the heterogeneous problem is linear), when both the solution and the coefficients are concerned. The homogenization procedure does not need necessarily any material periodicity, which is needed only for obtaining unique effective coefficients. Mathematical homogenization has been proved to be successful in many cases and will be adopted in the present paper. To quote only a very few works in this direction, let us mention Babuska (1976a), Babuska (1976b), Murat (1977), Tartar (1977), Bensoussan et al. (1978) and Sanchez-Palencia (1978). In many cases, mathematical homogenization gives explicit formulas for the effective parameters. More specifically, the explicit dependence of the effective parameters on the boundary and initial (if the problem is inelastic) conditions may be obtained. The boundary conditions-effect is related to the fundamental micromechanics problem.

The choice of a macroscopic constitutive model, whose material parameters are fitted into experimental data, is a decisive step to

* Corresponding author. Tel.: +30 2310995931; fax: +30 2310995679.
E-mail address: charalam@civil.auth.gr (N. Charalambakis).

0020-7683/$ - see front matter © 2009 Elsevier Ltd. All rights reserved.
doi:10.1016/j.ijsolstr.2009.07.015

predict the macroscopic response of heterogeneous materials. This model must then reflect some microstructural information. It could be interesting to look for the conditions under which a model has the same form at the phases' level too. This allows one to look for effective parameters (which then have a sense), and makes easier the mechanical characterization of heterogeneous materials. Generalizing this concept to the other governing equations, we will say that, if the equations of the limit problem are of the same type than the equations describing the heterogeneous material, then the problem is stable by homogenization (see also Charalambakis and Murat (2007)).

In this paper we study the homogenization of a pressurized hollow circular cylinder composed of elastic–perfectly plastic multilayered materials, with properties exhibiting discontinuities in the radial direction. The elastic and elastoplastic response of homogeneous and non-homogeneous thick- or thin-walled tubes under different boundary conditions was studied by Chatterjee (1970), Mukhopadhyay (1982), Geymonat et al. (1987a,b), and more recently investigated by Batra and Adulla (1995), Batra and Rattazi (1997), Horgan and Chan (1999a,b), Chen et al. (2000), Krishnaswamy and Beatty (2001), Tarn and Wang (2001), Burns and Davies, 2002, Tarn (2002b,a), Batra and Love (2004), Ruhi et al. (2005), Eraslan and Akis (2005), Batra and Lear (2005), Boussaa (2006) and Hosseini Kordkheili and Naghdabadi (2007). In many non-homogeneous cases the heterogeneities are assumed to obey defined smooth or continuous spatial variations. We note that in Chen et al. (2005) (see also Drago and Pindera (2007)) the effects of microstructural refinement and homogenization on the contact pressure and sub-surface stresses for the flat punch contact problem on periodically laminated multilayers were studied and the concept of partial homogenization was introduced leading to stress exhibiting very high stress gradients at the top layers. The problem of a tube made of cylindrically anisotropic elastic non-homogeneous periodic materials under axial force, torque at the ends, internal and external pressure, uniform in plane and antiplane shears on the inner and outer surfaces, was studied in Chatzigeorgiou et al. (2008) and turned out to be stable by homogenization.

In the present paper, we reformulate the incremental stress–total strain matrix relation, needed for this problem, for which the incremental stress–strain equations

$$\dot{\boldsymbol{\sigma}}^{\varepsilon} = \boldsymbol{C}^{e\varepsilon}\dot{\boldsymbol{\epsilon}}^{e\varepsilon} = \boldsymbol{C}^{e\varepsilon}(\dot{\boldsymbol{\epsilon}}^{\varepsilon} - \dot{\boldsymbol{\epsilon}}^{p\varepsilon}), \tag{1}$$

turn out to be not stable by homogenization, since the product $\boldsymbol{C}^{e\varepsilon}\dot{\boldsymbol{\epsilon}}^{p\varepsilon}$ does not converge to a product of effective matrices (Sections 2 and 3). Moreover, in Section 2, we show that even this new formulation allows for the manifestation of homogenization-induced anisotropy, if the non-homogeneous material is assumed to be isotropic. More specifically, regarding the incremental stress correction vector, we capture two effective plastic work-dependent parameters: one dependent on both elastic and plastic properties, having incremental stress dimension, and one dependent only on the plastic work, having incremental strain dimension. Combination of these parameters affects only the effective hoop and axial stresses, which both are not tractions. It is worth noticing that these effective parameters are independent. In Section 3 we present the homogenization of a cylindrically anisotropic tube. We find the effective elastic matrix and the effective incremental stress correction vector. Regarding the incremental stress correction vector, both non-homogeneous and homogenized materials exhibit three plastic work-dependent parameters, dependent also on the elastic, non-homogeneous and effective, respectively, parameters. Contrarily to the heterogeneous parameters, the effective plastic parameters are independent. Among these parameters, the first one is an incremental plastic strain-dimensioned parameter, while the second and the third parameters are incremental stress-dimensioned parameters. Only the first effective incremental plastic strain-like parameter enters into all effective incremental stresses. Moreover, in Section 4 we present numerical simulation of this problem, which is based on a modified "initial stress" finite differences method, inspired by the well known "initial stress" Finite Element Method (Zienkiewicz et al., 1969). Finally, in Section 5, two numerical examples confirm the theoretical findings.

2. Homogenization results for the isotropic non-homogeneous tube. Homogenization induced anisotropy

In the sequel, we refer to a long internally pressurized tube with axially constrained ends, having the section of Fig. 1, with the internal and external radii a and b, respectively. The length of the cylinder is sufficiently long with respect to its width that it allows one to consider a plain-strain problem. The only assumed displacement is the radial displacement $u_r^{\varepsilon} = u^{\varepsilon}$. Furthermore, it is assumed that the pressure p_i is increased so gradually that the tube is first deformed elastically. The tube is made of numerous isotropic layers of small thickness ε of very dissimilar materials. The parameter of heterogeneity ε enters to all functions. We will use polar coordinates r, θ, z, with the axis z along the axis of the tube. In incremental plasticity, the increment of total strain is divided in an elastic and a plastic part (Khan and Huang, 1995)

$$\dot{\epsilon}^{\varepsilon} = \dot{\epsilon}^{e\varepsilon} + \dot{\epsilon}^{p\varepsilon}, \tag{2}$$

where the dot over a function denotes partial derivative with time or, under the assumed slowly increasing pressure conditions, the increment of this function during a pseudo time. The incremental stress–strain relationships under plane strain conditions are

$$\begin{bmatrix} \dot{\sigma}_r^{\varepsilon} \\ \dot{\sigma}_{\theta}^{\varepsilon} \\ \dot{\sigma}_z^{\varepsilon} \end{bmatrix} = \begin{bmatrix} A^{\varepsilon} & A^{\varepsilon}N \\ A^{\varepsilon}N & A^{\varepsilon} \\ A^{\varepsilon}N & A^{\varepsilon}N \end{bmatrix} \begin{bmatrix} \dot{\epsilon}_r^{\varepsilon} - \dot{\epsilon}_r^{p\varepsilon} \\ \dot{\epsilon}_{\theta}^{\varepsilon} - \dot{\epsilon}_{\theta}^{p\varepsilon} \end{bmatrix}, \tag{3}$$

where

$$A^{\varepsilon}(r) = \frac{E^{\varepsilon}(r)(1 - \nu^{\varepsilon}(r))}{(1 + \nu^{\varepsilon}(r))(1 - 2\nu^{\varepsilon}(r))}, \quad N = \frac{\nu}{1 - \nu}, \tag{4}$$

are the elastic coefficients of the heterogeneous material ($E^{\varepsilon}(r)$ is the Young modulus and $\nu^{\varepsilon}(r)$ is the Poisson radio), which are assumed to exhibit discontinuities, being only bounded from above

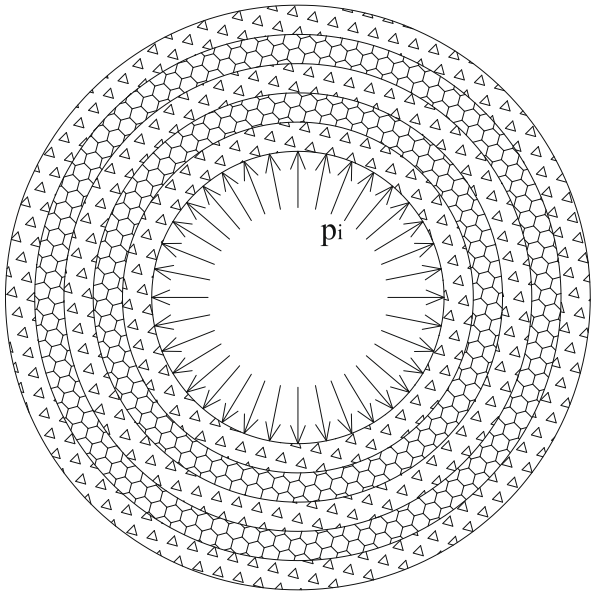

Fig. 1. Periodic material: internal pressure problem.

and from below by strictly positive constants. The same assumptions are valid for the yield limit in tension $\sigma_0^\varepsilon(r)$ of the heterogeneous material. Since the spatial variation in Poisson's ratio is of much less practical importance than that in Young's modulus, we assume that $v^\varepsilon(r)$ varies only in $A^\varepsilon(r)$. In the sequel, we will omit the dependence of functions on r, the index ε only being retained. The radial and angular incremental strains are given in terms of the radial incremental displacement

$$\dot{\epsilon}_r^\varepsilon = \frac{d\dot{u}^\varepsilon}{dr}, \quad \dot{\epsilon}_\theta^\varepsilon = \frac{\dot{u}^\varepsilon}{r}. \tag{5}$$

The equilibrium condition for the increments of stresses, using (3) and (5), reads

$$\frac{d\dot{\sigma}_r^\varepsilon}{dr} = \frac{\dot{\sigma}_\theta^\varepsilon - \dot{\sigma}_r^\varepsilon}{r} = -\frac{1-N}{r}\dot{\sigma}_r^\varepsilon + \frac{1-N^2}{r^2}A^\varepsilon \dot{u}^\varepsilon - \frac{1-N^2}{r}A^\varepsilon \dot{\epsilon}_\theta^{p\varepsilon}. \tag{6}$$

Moreover, from (3) and (5) we get

$$\dot{\epsilon}_r^\varepsilon = \frac{d\dot{u}^\varepsilon}{dr} = \frac{1}{A^\varepsilon}\dot{\sigma}_r^\varepsilon - \frac{N}{r}\dot{u}^\varepsilon + \dot{\epsilon}_r^{p\varepsilon} + N\dot{\epsilon}_\theta^{p\varepsilon}. \tag{7}$$

Eqs. (6) and (7) are accompanied by the boundary conditions

$$\dot{\sigma}_r^\varepsilon(a) = -\dot{p}_i, \quad \dot{\sigma}_r^\varepsilon(b) = 0. \tag{8}$$

It is worth noticing that the homogenization process does not need any continuity conditions. All unknown functions are allowed to be discontinuous in the space of bounded functions $L^\infty(a,b)$ and their convergence as $\varepsilon \to 0$ is studied. As it will be proved in the sequel, two of them, namely the radial normal stress and the radial displacement, converge strongly in the space of continuous functions as $\varepsilon \to 0$. Due to the fact that in all elastic regions (see Appendix B)

$$\sigma_\theta^\varepsilon > \sigma_z^\varepsilon > \sigma_r^\varepsilon, \tag{9}$$

the Tresca yield criterion for elastic–perfectly plastic material is

$$f^\varepsilon = \sigma_\theta^\varepsilon - \sigma_r^\varepsilon - \sigma_0^\varepsilon = \begin{cases} \text{negative}, & \dot{\epsilon}^{p\varepsilon} = 0, \\ 0, & \dot{\epsilon}^{p\varepsilon} \neq 0. \end{cases} \tag{10}$$

The flow rule for $f^\varepsilon = 0$ gives

$$\dot{\epsilon}_r^{p\varepsilon} = \dot{\lambda}^\varepsilon \frac{\partial f^\varepsilon}{\partial \sigma_r} = -\dot{\lambda}^\varepsilon, \quad \dot{\epsilon}_\theta^{p\varepsilon} = \dot{\lambda}^\varepsilon \frac{\partial f^\varepsilon}{\partial \sigma_\theta^\varepsilon} = \dot{\lambda}^\varepsilon, \quad \dot{\epsilon}_z^{p\varepsilon} = \dot{\lambda}^\varepsilon \frac{\partial f^\varepsilon}{\partial \sigma_z^\varepsilon} = 0, \tag{11}$$

where $\dot{\lambda}^\varepsilon$ is the non-homogeneous plastic work-dependent multiplier. These expressions for the plastic incremental strain components indicate that the material remains in the plane strain condition after the appearance of plastic deformation. The consistency condition for the plastic zones ($f^\varepsilon = \sigma_\theta^\varepsilon - \sigma_r^\varepsilon - \sigma_0^\varepsilon = 0$)

$$\dot{f}^\varepsilon = \dot{\sigma}_\theta^\varepsilon - \dot{\sigma}_r^\varepsilon = 0, \tag{12}$$

with the use of (3), (5), (7) and (11), leads to

$$0 < \dot{\lambda}^\varepsilon = \dot{\epsilon}_\theta^\varepsilon - \frac{1}{A^\varepsilon(1+N)}\dot{\sigma}_r^\varepsilon. \tag{13}$$

So, the non-homogeneous plastic work-dependent multiplier is given by

$$\dot{\lambda}^\varepsilon = \begin{cases} 0, & \dot{f}^\varepsilon \neq 0, \\ \frac{\dot{u}^\varepsilon}{r} - \frac{1}{1+N}\frac{1}{A^\varepsilon}\dot{\sigma}_r^\varepsilon, & \dot{f}^\varepsilon = 0. \end{cases} \tag{14}$$

From Eqs. (6), (7) and (11) we get

$$\begin{aligned} \frac{d\dot{\sigma}_r^\varepsilon}{dr} &= -\frac{1-N}{r}\dot{\sigma}_r^\varepsilon + \frac{1-N^2}{r^2}A^\varepsilon \dot{u}^\varepsilon - \frac{1-N^2}{r}A^\varepsilon \dot{\lambda}^\varepsilon, \\ \frac{d\dot{u}^\varepsilon}{dr} &= \frac{1}{A^\varepsilon}\dot{\sigma}_r^\varepsilon - \frac{N}{r}\dot{u}^\varepsilon - (1-N)\dot{\lambda}^\varepsilon, \end{aligned} \tag{15}$$

or, by using (13),

$$\begin{aligned} \frac{d\dot{\sigma}_r^\varepsilon}{dr} &= \begin{cases} -\frac{1-N}{r}\dot{\sigma}_r^\varepsilon + \frac{1-N^2}{r^2}A^\varepsilon \dot{u}^\varepsilon, & \dot{\lambda}^\varepsilon = 0, \\ 0, & \dot{\lambda}^\varepsilon > 0, \end{cases} \\ \frac{d\dot{u}^\varepsilon}{dr} &= \begin{cases} (1/A^\varepsilon)\dot{\sigma}_r^\varepsilon - N\dot{u}^\varepsilon/r, & \dot{\lambda}^\varepsilon = 0, \\ \frac{2/A^\varepsilon}{(1+N)}\dot{\sigma}_r^\varepsilon - \dot{u}^\varepsilon/r, & \dot{\lambda}^\varepsilon > 0, \end{cases} \end{aligned} \tag{16}$$

while from Eqs. (3) and (11) we get

$$\begin{aligned} \dot{\sigma}_r^\varepsilon &= A^\varepsilon \frac{d\dot{u}^\varepsilon}{dr} + NA^\varepsilon \frac{\dot{u}^\varepsilon}{r} + (1-N)A^\varepsilon \dot{\lambda}^\varepsilon, \\ \dot{\sigma}_\theta^\varepsilon &= NA^\varepsilon \frac{d\dot{u}^\varepsilon}{dr} + A^\varepsilon \frac{\dot{u}^\varepsilon}{r} - (1-N)A^\varepsilon \dot{\lambda}^\varepsilon, \\ \dot{\sigma}_z^\varepsilon &= v(\dot{\sigma}_r^\varepsilon + \dot{\sigma}_\theta^\varepsilon). \end{aligned} \tag{17}$$

Additionally, $\dot{\sigma}_\theta^\varepsilon$ is written

$$\dot{\sigma}_\theta^\varepsilon = N\dot{\sigma}_r^\varepsilon + (1-N^2)A^\varepsilon \frac{\dot{u}^\varepsilon}{r} - (1-N^2)A^\varepsilon \dot{\lambda}^\varepsilon. \tag{18}$$

The system of linear differential equations (15) or (16) with boundary conditions (8) is similar to the system studied in Chatzigeorgiou et al. (2008), provided that continuity conditions for $\dot{\sigma}_r^\varepsilon$ and $\dot{u}_r^\varepsilon$ at the common points of elastic and plastic regions during every incremental loading are added. Due to the weak formulation of the first order differential equations (16), describing the heterogeneous problem, one cannot obtain a second order ordinary differential equation in the radial displacement before proving the compactness of radial stress and displacement (i.e. the boundness of these functions and of their first derivatives). In other words, the term $(1/A^\varepsilon)\dot{\sigma}_r^\varepsilon$ in the second equation of (16) cannot be differentiated as a product in order to be combined with the first equation of (16) and give a second order ordinary differential equation in the radial displacement.

Following parallel lines with Chatzigeorgiou et al. (2008), we can prove (see Appendix A) that $\dot{\sigma}_r^\varepsilon$ and $\dot{u}_r^\varepsilon$ converge strongly in the space of continuous functions $C(a,b)$. Recalling (17), (18), (5) and (11), we can show that all the other incremental stress and all incremental strain components converge weakly in the space $L^\infty(a,b)$ of bounded functions. We now define

$$\dot{\Lambda}^\varepsilon = A^\varepsilon \dot{\lambda}^\varepsilon = A^\varepsilon \frac{\dot{u}^\varepsilon}{r} - \frac{1}{(1+N)}\dot{\sigma}_r^\varepsilon. \tag{19}$$

We will verify that this is one of the two plastic coefficients whose limit enters in the expressions of the weakly convergent incremental stress components $\dot{\sigma}_\theta^\varepsilon$ and $\dot{\sigma}_z^\varepsilon$ in (17) when the non-homogeneous parameter ε tends to zero.

In the sequel, we denote by $\langle \phi^\varepsilon \rangle$ the mean value of a periodic function ϕ^ε and by ψ^h the weak limit in the space of bounded functions of the sequences ψ^ε when $\varepsilon \to 0$.

Since $\dot{\sigma}_r^\varepsilon$ and $\dot{u}^\varepsilon$ converge strongly, we can pass to the limit in the linear equations (15) and obtain the differential equations of the homogenized material

$$\begin{aligned} \frac{d\dot{\sigma}_r^h}{dr} &= -\frac{1-N}{r}\dot{\sigma}_r^h + \frac{1-N^2}{r^2}\langle A^\varepsilon \rangle \dot{u}^h - \frac{1-N^2}{r}\dot{\Lambda}^h, \\ \frac{d\dot{u}^h}{dr} &= \left\langle \frac{1}{A^\varepsilon} \right\rangle \dot{\sigma}_r^h - \frac{N}{r}\dot{u}^h - (1-N)\dot{\lambda}^h, \end{aligned} \tag{20}$$

where from (13) and (19) and by passing to the limit we have

$$\dot{\lambda}^h = \frac{\dot{u}^h}{r} - \frac{1}{(1+N)}\left\langle \frac{1}{A^\varepsilon} \right\rangle \dot{\sigma}_r^h, \quad \dot{\Lambda}^h = \langle A^\varepsilon \rangle \frac{\dot{u}^h}{r} - \frac{1}{(1+N)}\dot{\sigma}_r^h. \tag{21}$$

Passing to the limit in (17), with the help of the second equation (20) and (18), gives the incremental stress components of the homogenized material in terms of the displacement and two plastic parameters $\dot{\lambda}^h$ and $\dot{\Lambda}^h$,

$$\begin{aligned}\dot{\sigma}_r^h &= \frac{1}{\langle 1/A^\varepsilon\rangle}\frac{d\dot{u}^h}{dr} + \frac{N}{\langle 1/A^\varepsilon\rangle}\frac{\dot{u}^h}{r} + \frac{1-N}{\langle 1/A^\varepsilon\rangle}\dot{\lambda}^h,\\ \dot{\sigma}_\theta^h &= \frac{N}{\langle 1/A^\varepsilon\rangle}\frac{d\dot{u}^h}{dr} + \frac{N^2+(1-N^2)\langle A^\varepsilon\rangle\langle 1/A^\varepsilon\rangle}{\langle 1/A^\varepsilon\rangle}\frac{\dot{u}^h}{r}\\ &\quad - \frac{(1-N^2)\langle 1/A^\varepsilon\rangle\dot{\Lambda}^h + (N^2-N)\dot{\lambda}^h}{\langle 1/A^\varepsilon\rangle},\\ \dot{\sigma}_z^h &= \nu(\dot{\sigma}_r^h + \dot{\sigma}_\theta^h).\end{aligned} \tag{22}$$

Comparing (17) with (22) reveals that the homogenized material exhibits elastic and plastic anisotropy. Concerning the elastic anisotropy, we refer to Chatzigeorgiou et al. (2008). Concerning the plastic anisotropy, it is worth noticing that, contrarily to $\dot{\lambda}^h$, which is a quantity of the order of small incremental plastic strain, the homogenization-induced coefficient $\dot{\Lambda}^h$ is measured like an incremental stress. Although both the non-homogeneous and the homogenized plastic incremental strain components are defined exclusively from $\dot{\lambda}^\varepsilon$ and $\dot{\lambda}^h$, respectively, the expressions for the stresses differ: the stresses of the non-homogeneous material depend exclusively on one plastic work-dependent parameter $\dot{\Lambda}^\varepsilon$, while the effective stresses depend on two independent effective plastic work-dependent parameters $\dot{\lambda}^h$ and $\dot{\Lambda}^h$. A final observation is that, although in the non-homogeneous material $\dot{\sigma}_z^\varepsilon$ depends only implicitly on the incremental plastic strain $\dot{\lambda}^\varepsilon$, in the homogenized material $\dot{\sigma}_z^h$ depends explicitly on the effective incremental plastic strain $\dot{\lambda}^h$. The homogenized yield criterion f^h, the homogenized consistency equation, the homogenized incremental total $\dot{\epsilon}_r^h, \dot{\epsilon}_\theta^h$ and plastic $\dot{\epsilon}_r^{ph}, \dot{\epsilon}_\theta^{ph}$ strains can be obtained directly by passing to the limit in the linear equations (10), (12), (5) and (11), respectively,

$$f^h = \sigma_\theta^h - \sigma_r^h - \langle\sigma_0^\varepsilon\rangle = \begin{cases} \neq 0, & \dot{\epsilon}^{ph} = 0,\\ 0, & \dot{\epsilon}^{ph} \neq 0,\end{cases} \tag{23}$$

$$\dot{f}^h = \dot{\sigma}_\theta^h - \dot{\sigma}_r^h = 0, \tag{24}$$

$$\dot{\epsilon}_r^h = \frac{d\dot{u}^h}{dr}, \quad \dot{\epsilon}_\theta^h = \frac{\dot{u}^h}{r}, \tag{25}$$

$$\dot{\epsilon}_r^{ph} = -\dot{\lambda}^h, \quad \dot{\epsilon}_\theta^{ph} = \dot{\lambda}^h, \quad \dot{\epsilon}_z^{ph} = 0. \tag{26}$$

It is worth noticing that the choice of the linear Tresca yield criterion allows one to pass directly to the limit in (12) and obtain (24). It would not be so easy if the more general, nonlinear, Von Mises criterion were used.

Moreover, we observe that a new matrix formulation is needed: the total incremental strain in (1) needs to be separated from the plastic incremental strain, since, for the homogenized material, there is no longer a limiting matrix like $\mathbf{C}^{e\varepsilon}$ as in the non-homogeneous material. This is due to the fact that we cannot pass to the limit in (3), where all functions, except $\dot{\sigma}_r^\varepsilon$, converge weakly. This alternative formulation starts from a new matrix formulation of the non-homogeneous material between incremental stress and incremental total strain in the form

$$\begin{bmatrix}\dot{\sigma}_r^\varepsilon\\ \dot{\sigma}_\theta^\varepsilon\\ \dot{\sigma}_z^\varepsilon\end{bmatrix} = \begin{bmatrix}A^\varepsilon & A^\varepsilon N\\ A^\varepsilon N & A^\varepsilon\\ A^\varepsilon N & A^\varepsilon N\end{bmatrix}\begin{bmatrix}\frac{d\dot{u}^\varepsilon}{dr}\\ \\ \frac{\dot{u}^\varepsilon}{r}\end{bmatrix} + \begin{bmatrix}(1-N)\dot{\lambda}^\varepsilon A^\varepsilon\\ -(1-N)\dot{\lambda}^\varepsilon A^\varepsilon\\ 0\end{bmatrix}. \tag{27}$$

In this form the incremental stress is divided into two parts: the first is computed elastically from the total strain, while the second, herein named "correction stress vector", is computed "plastically" using the work-dependent parameter $\dot{\Lambda}^\varepsilon$ at every incremental load. Now the incremental stress–strain relation is stable by homogenization and the corresponding homogenized form obtained from (22) reads

$$\begin{aligned}\begin{bmatrix}\dot{\sigma}_r^h\\ \dot{\sigma}_\theta^h\\ \dot{\sigma}_z^h\end{bmatrix} &= \begin{bmatrix}\frac{1}{\langle 1/A^\varepsilon\rangle} & \frac{N}{\langle 1/A^\varepsilon\rangle}\\ \frac{N}{\langle 1/A^\varepsilon\rangle} & \frac{N^2}{\langle 1/A^\varepsilon\rangle} + (1-N^2)\langle A^\varepsilon\rangle\\ \frac{N}{\langle 1/A^\varepsilon\rangle} & \frac{N^2}{\langle 1/A^\varepsilon\rangle} + (N-N^2)\langle A^\varepsilon\rangle\end{bmatrix}\begin{bmatrix}\frac{d\dot{u}^h}{dr}\\ \\ \frac{\dot{u}^h}{r}\end{bmatrix}\\ &\quad + \begin{bmatrix}(1-N)\frac{1}{\langle 1/A^\varepsilon\rangle}\dot{\lambda}^h\\ N(1-N)\frac{1}{\langle 1/A^\varepsilon\rangle}\dot{\lambda}^h - (1-N^2)\dot{\Lambda}^h\\ N(1-N)\frac{1}{\langle 1/A^\varepsilon\rangle}\dot{\lambda}^h - (N-N^2)\dot{\Lambda}^h\end{bmatrix}.\end{aligned} \tag{28}$$

It is worth noticing that, although $\dot{\Lambda}^\varepsilon$ can be calculated from $\dot{\lambda}^\varepsilon$ in the non-homogeneous material (see (19)), the effective $\dot{\Lambda}^h$ is independent of $\dot{\lambda}^h$. The two effective plastic work-dependent parameters coexist in the incremental stress correction vector without communicating, manifesting a kind of homogenization-induced plastic anisotropy. We can finally find the error of using (1) for the calculation of the effective incremental stress correction vector. In this case, the "homogenized" form reads

$$\begin{bmatrix}\dot{\sigma}_r^h\\ \dot{\sigma}_\theta^h\\ \dot{\sigma}_z^h\end{bmatrix} = \begin{bmatrix}\frac{1}{\langle 1/A^\varepsilon\rangle} & \frac{N}{\langle 1/A^\varepsilon\rangle}\\ \frac{N}{\langle 1/A^\varepsilon\rangle} & \frac{N^2}{\langle 1/A^\varepsilon\rangle} + (1-N^2)\langle A^\varepsilon\rangle\\ \frac{N}{1/A^\varepsilon} & \frac{N^2}{\langle 1/A^\varepsilon\rangle} + (N-N^2)\langle A^\varepsilon\rangle\end{bmatrix}\begin{bmatrix}\frac{d\dot{u}^h}{dr} + \frac{N}{\langle A^\varepsilon\rangle}\dot{\Lambda}^h + (1-N)\dot{\lambda}^h\\ \\ \frac{\dot{u}^h}{r} - \frac{\dot{\lambda}^h}{\langle A^\varepsilon\rangle}\end{bmatrix}, \tag{29}$$

from which and using (21) it follows that the sum of incremental plastic strains is not zero

$$\begin{aligned}\frac{N}{\langle A^\varepsilon\rangle}\dot{\Lambda}^h + (1-N)\dot{\lambda}^h - \frac{\dot{\Lambda}^h}{\langle A^\varepsilon\rangle} &= (1-N)\left(\dot{\lambda}^h - \frac{\dot{\Lambda}^h}{\langle A^\varepsilon\rangle}\right)\\ &= \frac{1-N}{1+N}\dot{\sigma}_r\left(\frac{1}{\langle A^\varepsilon\rangle} - \left\langle\frac{1}{A^\varepsilon}\right\rangle\right).\end{aligned} \tag{30}$$

But this is not a correct result, the (incorrectly) "homogenized" material being no longer plastically incompressible.

3. Homogenization of cylindrically orthotropic non-homogeneous materials

We now consider the special case of anisotropic material exhibiting elastic cylindrical anisotropy and plastic anisotropy. The incremental stress–strain matrix form reads

$$\dot{\boldsymbol{\sigma}}^\varepsilon = \mathbf{C}^{e\varepsilon}\dot{\boldsymbol{\epsilon}}^\varepsilon + \dot{\boldsymbol{\sigma}}^{p\varepsilon}, \tag{31}$$

where $\mathbf{C}^{e\varepsilon}$ is the elastic matrix, given by

$$\mathbf{C}^{e\varepsilon} = \begin{bmatrix}C_{11}^\varepsilon & C_{12}^\varepsilon\\ C_{12}^\varepsilon & C_{22}^\varepsilon\\ C_{13}^\varepsilon & C_{23}^\varepsilon\end{bmatrix}, \tag{32}$$

and $\dot{\boldsymbol{\sigma}}^{p\varepsilon}$ is the incremental stress correction vector given by

$$\dot{\boldsymbol{\sigma}}^{p\varepsilon} = -\mathbf{C}^{e\varepsilon}\dot{\boldsymbol{\epsilon}}^{p\varepsilon}. \tag{33}$$

In the literature there are several generalizations of the Tresca anisotropic yield criterion (Lemaitre, 2001). Here we adopt the anisotropic Tresca yield criterion in Berman and Hodge (1959),

$$\begin{aligned}&\frac{\sigma_r^\varepsilon - \sigma_\theta^\varepsilon}{a^\varepsilon} = 1, \quad \frac{\sigma_\theta^\varepsilon - \sigma_z^\varepsilon}{b^\varepsilon} = 1, \quad \frac{\sigma_z^\varepsilon - \sigma_r^\varepsilon}{c^\varepsilon} = 1,\\ &\frac{\sigma_\theta^\varepsilon - \sigma_r^\varepsilon}{d^\varepsilon} = 1, \quad \frac{\sigma_z^\varepsilon - \sigma_\theta^\varepsilon}{e^\varepsilon} = 1, \quad \frac{\sigma_r^\varepsilon - \sigma_z^\varepsilon}{g^\varepsilon} = 1,\end{aligned} \tag{34}$$

where $a^\varepsilon, b^\varepsilon, c^\varepsilon, d^\varepsilon, e^\varepsilon, g^\varepsilon$ are material parameters. This yield criterion, together with (9), leads to the anisotropic flow rule

$$\dot{\epsilon}_r^{p\varepsilon} = \dot{\lambda}_1^\varepsilon\frac{\partial f^\varepsilon}{\partial\sigma_r} = -\dot{\lambda}_1^\varepsilon, \quad \dot{\epsilon}_\theta^{p\varepsilon} = \dot{\lambda}_2^\varepsilon\frac{\partial f^\varepsilon}{\partial\sigma_\theta^\varepsilon} = \dot{\lambda}_2^\varepsilon, \quad \dot{\epsilon}_z^{p\varepsilon} = \dot{\lambda}_3^\varepsilon\frac{\partial f^\varepsilon}{\partial\sigma_z^\varepsilon} = 0. \tag{35}$$

Then, using the incompressibility condition we deduce that, necessarily

$$\dot{\lambda}_1^\varepsilon = \dot{\lambda}_2^\varepsilon = \dot{\lambda}^\varepsilon. \tag{36}$$

We conclude that the plastic flow is isotropic. The isotropy of the plastic flow is a necessary result of the choice of Tresca yield criterion, which implies that the z-component of the incremental plastic strain is equal to zero, and of the incompressibility, which implies that the two other components are equal to $\pm\dot{\lambda}^\varepsilon$. The potential use of Von Mises criterion is less restrictive at this point and may allow three incremental plastic strain components, dependent on three plastic coefficients $\dot{\lambda}_1^\varepsilon, \dot{\lambda}_2^\varepsilon, \dot{\lambda}_3^\varepsilon$ having a sum equal to zero.

Then the incremental stress correction vector $\dot{\boldsymbol{\sigma}}^{p\varepsilon}$ is given by

$$\dot{\boldsymbol{\sigma}}^{p\varepsilon} = \begin{bmatrix} (C_{11}^\varepsilon - C_{12}^\varepsilon)\dot{\lambda}^\varepsilon \\ (C_{12}^\varepsilon - C_{22}^\varepsilon)\dot{\lambda}^\varepsilon \\ (C_{13}^\varepsilon - C_{23}^\varepsilon)\dot{\lambda}^\varepsilon \end{bmatrix}, \tag{37}$$

therefore

$$\begin{bmatrix} \dot{\sigma}_r^\varepsilon \\ \dot{\sigma}_\theta^\varepsilon \\ \dot{\sigma}_z^\varepsilon \end{bmatrix} = \begin{bmatrix} C_{11}^\varepsilon & C_{12}^\varepsilon \\ C_{12}^\varepsilon & C_{22}^\varepsilon \\ C_{13}^\varepsilon & C_{23}^\varepsilon \end{bmatrix} \begin{bmatrix} \frac{d\dot{u}^\varepsilon}{dr} \\ \frac{\dot{u}^\varepsilon}{r} \end{bmatrix} + \begin{bmatrix} (C_{11}^\varepsilon - C_{12}^\varepsilon)\dot{\lambda}^\varepsilon \\ (C_{12}^\varepsilon - C_{22}^\varepsilon)\dot{\lambda}^\varepsilon \\ (C_{13}^\varepsilon - C_{23}^\varepsilon)\dot{\lambda}^\varepsilon \end{bmatrix}, \tag{38}$$

where the elastic coefficients C_{11}^ε, C_{12}^ε, C_{22}^ε, C_{13}^ε and C_{23}^ε are allowed to exhibit discontinuities, being only bounded from above and from below by strictly positive functions. We make the following additional assumptions on the anisotropic elastic coefficients:

$$\begin{aligned} &C_{11}^\varepsilon(r) > C_{13}^\varepsilon(r), \quad C_{22}^\varepsilon(r) > C_{23}^\varepsilon(r), \quad C_{13}^\varepsilon(r) \geqslant C_{12}^\varepsilon(r), \\ &C_{23}^\varepsilon(r) \geqslant C_{12}^\varepsilon(r), \qquad \forall r,\ a \leqslant r \leqslant b, \end{aligned} \tag{39}$$

which are sufficient to ensure that equation (9) holds. We also make the following physically justifiable assumptions:

$$C_{11}^\varepsilon(r) > C_{12}^\varepsilon(r), \quad C_{11}^\varepsilon(r)C_{22}^\varepsilon(r) - \left(C_{12}^\varepsilon(r)\right)^2 > 0, \qquad \forall r,\ a \leqslant r \leqslant b, \tag{40}$$

which are sufficient to ensure that $\dot{\sigma}_r^\varepsilon, \frac{d\dot{\sigma}_r^\varepsilon}{dr}, \dot{u}^\varepsilon, \frac{d\dot{u}^\varepsilon}{dr}$ are bounded in $L^\infty(a,b)$ independently of ε, as long as the tube is deformed elastically (Chatzigeorgiou et al., 2008). Then, by assuming continuity for $\dot{\sigma}_r^\varepsilon$ and $\dot{u}^\varepsilon$ at all points between elastic and plastic regions, we can follow the same lines as in Chatzigeorgiou et al. (2008) and prove that

$$\dot{u}^\varepsilon \to \dot{u}^h \text{ in } C(a,b), \quad \dot{\sigma}_r^\varepsilon \to \dot{\sigma}_r^h \text{ in } C(a,b). \tag{41}$$

Then, from the first equation of (38) we obtain

$$\frac{d\dot{u}^\varepsilon}{dr} = \frac{1}{C_{11}^\varepsilon}\dot{\sigma}_r^\varepsilon - \frac{C_{12}^\varepsilon}{C_{11}^\varepsilon}\frac{\dot{u}^\varepsilon}{r} - \left(1 - \frac{C_{12}^\varepsilon}{C_{11}^\varepsilon}\right)\dot{\lambda}^\varepsilon. \tag{42}$$

We now put

$$\dot{\Lambda}_1^\varepsilon = \left(1 - \frac{C_{12}^\varepsilon}{C_{11}^\varepsilon}\right)\dot{\lambda}^\varepsilon \tag{43}$$

and using (41) we can pass to the limit in (42) and obtain

$$\frac{d\dot{u}^h}{dr} = \left\langle \frac{1}{C_{11}^\varepsilon} \right\rangle \dot{\sigma}_r^h - \left\langle \frac{C_{12}^\varepsilon}{C_{11}^\varepsilon} \right\rangle \frac{\dot{u}^h}{r} - \dot{\Lambda}_1^h, \tag{44}$$

where

$$\dot{\Lambda}_1^\varepsilon = \left(1 - \frac{C_{12}^\varepsilon}{C_{11}^\varepsilon}\right)\dot{\lambda}^\varepsilon \rightharpoonup \dot{\Lambda}_1^h \quad \text{in } L^\infty(a,b). \tag{45}$$

Consistency equation $\dot{\sigma}_r^\varepsilon = \dot{\sigma}_\theta^\varepsilon$ together with the first and the second of equations (38) and (42) give the expression of the plastic work-dependent non-homogeneous parameter

$$\dot{\lambda}^\varepsilon = \frac{\dot{u}^\varepsilon}{r} - \frac{C_{11}^\varepsilon - C_{12}^\varepsilon}{C_{11}^\varepsilon C_{22}^\varepsilon - \left(C_{12}^\varepsilon\right)^2}\dot{\sigma}_r^\varepsilon. \tag{46}$$

Recalling (41) the homogenized incremental plastic strain can now be obtained by passing to the limit in (46) thus obtaining

$$\dot{\lambda}^h = \frac{\dot{u}^h}{r} - \left\langle \frac{C_{11}^\varepsilon - C_{12}^\varepsilon}{C_{11}^\varepsilon C_{22}^\varepsilon - \left(C_{12}^\varepsilon\right)^2} \right\rangle \dot{\sigma}_r^h. \tag{47}$$

Moreover, we can define $\dot{\Lambda}_1^h$ from (46) and (45) by passing to the limit in terms of $\dot{u}^h$ and $\dot{\sigma}_r^h$,

$$\dot{\Lambda}_1^\varepsilon = \frac{C_{11}^\varepsilon - C_{12}^\varepsilon}{C_{11}^\varepsilon}\frac{\dot{u}^\varepsilon}{r} - \frac{\left(C_{11}^\varepsilon - C_{12}^\varepsilon\right)^2}{C_{11}(C_{11}^\varepsilon C_{22}^\varepsilon - \left(C_{12}^\varepsilon\right)^2)}\dot{\sigma}_r^\varepsilon, \tag{48}$$

obtaining

$$\dot{\Lambda}_1^h = \left\langle \frac{C_{11}^\varepsilon - C_{12}^\varepsilon}{C_{11}^\varepsilon} \right\rangle \frac{\dot{u}^h}{r} - \left\langle \frac{\left(C_{11}^\varepsilon - C_{12}^\varepsilon\right)^2}{C_{11}(C_{11}^\varepsilon C_{22}^\varepsilon - \left(C_{12}^\varepsilon\right)^2)} \right\rangle \dot{\sigma}_r^h. \tag{49}$$

Using the second equation of (38) and (42) we obtain

$$\dot{\sigma}_\theta^\varepsilon = \frac{C_{12}^\varepsilon}{C_{11}^\varepsilon}\dot{\sigma}_r^\varepsilon + \frac{C_{11}^\varepsilon C_{22}^\varepsilon - \left(C_{12}^\varepsilon\right)^2}{C_{11}^\varepsilon}\frac{\dot{u}^\varepsilon}{r} - \frac{C_{11}^\varepsilon C_{22}^\varepsilon - \left(C_{12}^\varepsilon\right)^2}{C_{11}^\varepsilon}\dot{\lambda}^\varepsilon. \tag{50}$$

Similarly, from the third equation of (38) and (42),

$$\dot{\sigma}_z^\varepsilon = \frac{C_{13}^\varepsilon}{C_{11}^\varepsilon}\dot{\sigma}_r^\varepsilon + \frac{C_{11}^\varepsilon C_{23}^\varepsilon - C_{12}^\varepsilon C_{13}^\varepsilon}{C_{11}^\varepsilon}\frac{\dot{u}^\varepsilon}{r} - \frac{C_{11}^\varepsilon C_{23}^\varepsilon - C_{12}^\varepsilon C_{13}^\varepsilon}{C_{11}^\varepsilon}\dot{\lambda}^\varepsilon. \tag{51}$$

We next define

$$\dot{\Lambda}_2^\varepsilon = \frac{C_{11}^\varepsilon C_{22}^\varepsilon - \left(C_{12}^\varepsilon\right)^2}{C_{11}^\varepsilon}\dot{\lambda}^\varepsilon \tag{52}$$

and

$$\dot{\Lambda}_3^\varepsilon = \frac{C_{11}^\varepsilon C_{23}^\varepsilon - C_{12}^\varepsilon C_{13}^\varepsilon}{C_{11}^\varepsilon}\dot{\lambda}^\varepsilon, \tag{53}$$

which, owing to (46), permit to pass to the limit and obtain $\dot{\Lambda}_2^h$ and $\dot{\Lambda}_3^h$ in terms of $\dot{u}^h$ and $\dot{\sigma}_r^h$,

$$\dot{\Lambda}_2^h = \left\langle \frac{C_{11}^\varepsilon C_{22}^\varepsilon - \left(C_{12}^\varepsilon\right)^2}{C_{11}^\varepsilon} \right\rangle \frac{\dot{u}^h}{r} - \left\langle \frac{C_{11}^\varepsilon - C_{12}^\varepsilon}{C_{11}^\varepsilon} \right\rangle \dot{\sigma}_r^h, \tag{54}$$

$$\dot{\Lambda}_3^h = \left\langle \frac{C_{11}^\varepsilon C_{23}^\varepsilon - C_{12}^\varepsilon C_{13}^\varepsilon}{C_{11}^\varepsilon} \right\rangle \frac{\dot{u}^h}{r} - \left\langle \frac{\left(C_{11}^\varepsilon - C_{12}^\varepsilon\right)\left(C_{11}^\varepsilon C_{23}^\varepsilon - C_{12}^\varepsilon C_{13}^\varepsilon\right)}{C_{11}^\varepsilon(C_{11}^\varepsilon C_{22}^\varepsilon - \left(C_{12}^\varepsilon\right)^2)} \right\rangle \dot{\sigma}_r^h. \tag{55}$$

From (44) and (45) we find the effective incremental radial stress $\dot{\sigma}_r^h$:

$$\dot{\sigma}_r^h = \frac{1}{\langle 1/C_{11}^\varepsilon \rangle}\frac{d\dot{u}^h}{dr} + \frac{\langle C_{12}^\varepsilon/C_{11}^\varepsilon \rangle}{\langle 1/C_{11}^\varepsilon \rangle}\frac{\dot{u}^h}{r} + \frac{\dot{\Lambda}_1^h}{\langle 1/C_{11}^\varepsilon \rangle}. \tag{56}$$

Then, using respectively (50), (52) and (51), (53) and passing to the limit we obtain the remaining effective incremental stresses

$$\begin{aligned} \dot{\sigma}_\theta^h = {} & \frac{\langle C_{12}^\varepsilon/C_{11}^\varepsilon \rangle}{\langle 1/C_{11}^\varepsilon \rangle}\frac{d\dot{u}^h}{dr} + \left[\frac{\langle C_{12}^\varepsilon/C_{11}^\varepsilon \rangle^2}{\langle 1/C_{11}^\varepsilon \rangle} + \left\langle \frac{C_{11}^\varepsilon C_{22}^\varepsilon - \left(C_{12}^\varepsilon\right)^2}{C_{11}^\varepsilon} \right\rangle\right]\frac{\dot{u}^h}{r} \\ & - \dot{\Lambda}_2^h + \frac{\langle C_{12}^\varepsilon/C_{11}^\varepsilon \rangle}{\langle 1/C_{11}^\varepsilon \rangle}\dot{\Lambda}_1^h, \end{aligned} \tag{57}$$

$$\begin{aligned} \dot{\sigma}_z^h = {} & \frac{\langle C_{13}^\varepsilon/C_{11}^\varepsilon \rangle}{\langle 1/C_{11}^\varepsilon \rangle}\frac{d\dot{u}^h}{dr} + \left[\frac{\langle C_{13}^\varepsilon/C_{11}^\varepsilon \rangle\langle C_{12}^\varepsilon/C_{11}^\varepsilon \rangle}{\langle 1/C_{11}^\varepsilon \rangle} + \left\langle \frac{C_{11}^\varepsilon C_{23}^\varepsilon - C_{12}^\varepsilon C_{13}^\varepsilon}{C_{11}^\varepsilon} \right\rangle\right]\frac{\dot{u}^h}{r} \\ & + \frac{\langle C_{13}^\varepsilon/C_{11}^\varepsilon \rangle}{\langle 1/C_{11}^\varepsilon \rangle}\dot{\Lambda}_1^h - \dot{\Lambda}_3^h. \end{aligned} \tag{58}$$

We conclude that the effective elastic matrix reads

$$\dot{\mathbf{C}}^{eh}=\begin{bmatrix}\frac{1}{\langle 1/C^e_{11}\rangle} & \frac{\langle C^e_{12}/C^e_{11}\rangle}{\langle 1/C^e_{11}\rangle}\\ \frac{\langle C^e_{12}/C^e_{11}\rangle}{\langle 1/C^e_{11}\rangle} & \frac{\langle C^e_{12}/C^e_{11}\rangle^2}{\langle 1/C^e_{11}\rangle}+\left\langle\frac{C^e_{11}C^e_{22}-\left(C^e_{12}\right)^2}{C^e_{11}}\right\rangle\\ \frac{\langle C^e_{13}/C^e_{11}\rangle}{\langle 1/C^e_{11}\rangle} & \frac{\langle C^e_{12}/C^e_{11}\rangle\langle C^e_{13}/C^e_{11}\rangle}{\langle 1/C^e_{11}\rangle}+\left\langle\frac{C^e_{11}C^e_{23}-C^e_{12}C^e_{13}}{C^e_{11}}\right\rangle\end{bmatrix}, \tag{59}$$

and that the effective incremental stress correction matrix reads

$$\dot{\boldsymbol{\sigma}}^{ph}=\begin{bmatrix}\frac{\dot{\Lambda}^h_1}{\langle 1/C^e_{11}\rangle}\\ \frac{\langle C^e_{12}/C^e_{11}\rangle}{\langle 1/C^e_{11}\rangle}\dot{\Lambda}^h_1-\dot{\Lambda}^h_2\\ \frac{\langle C^e_{13}/C^e_{11}\rangle}{\langle 1/C^e_{11}\rangle}\dot{\Lambda}^h_1-\dot{\Lambda}^h_3\end{bmatrix}, \tag{60}$$

in which $\dot{\Lambda}^h_1$ is an incremental strain-dimensioned quantity, while $\dot{\Lambda}^h_2$ and $\dot{\Lambda}^h_3$ are incremental stress-dimensioned quantities. All these effective quantities are independent.

The properties of the homogenized material depend on the equations considered for homogenization. In this paper, we consider the governing equations, including the constitutive incremental equation, written in an appropriate way. The constitutive equation, written in the form (1), contains the term $\mathbf{C}^{e\varepsilon}\dot{\boldsymbol{\epsilon}}^{p\varepsilon}$, which is the term of two weakly convergent terms, so it cannot converge to a product. Constitutive equation (1) cannot preserves the product $\mathbf{C}^{e\varepsilon}\dot{\boldsymbol{\epsilon}}^{p\varepsilon}$ in its effective form, so it is not stable by homogenization. In the present study, we show that, in the case of a multilayered tube under pressure, the incremental stress–strain relation of the effective medium can be expressed with an effective elastic stiffness matrix and an incremental stress correction vector. In Hill's micromechanics approach (Hill, 1965) the incremental stress–strain relation of the effective medium is given in terms of an effective *tangent modulus*. In such an approach there is no separation between the elastic and plastic behavior of the homogenized material. In the present work, we quantify the elastic and plastic anisotropic behavior of the effective medium. The effective elastic stiffness matrix presents orthotropic behavior, while the effective incremental stress correction vector contains two (if the constituent layers are isotropic) or three (if the constituent layers are orthotropic) plastic work-dependent parameters.

Our result can be compared with conclusions in Qu and Cherkaoui (2006), where micromechanics methods for linear behavior and the related approaches of Hill, Kroner and other researches are presented. It is reported there that the rate of elastic and plastic rate in the effective material cannot be produced by ensemble averaging the corresponding heterogeneous quantities. In the present work, in view of looking for effective incremental constitutive relations (31), we sacrifice (1) (equivalently (2)), which is not valid in the effective material.

Finally, concerning the stress correction vector, we note that Khatam and Pindera (2009) used this concept for the total stress–strain relations.

4. Numerical simulation

The numerical simulation is a modified "stress correction" finite difference method, based on the "initial stress" finite element method described in Zienkiewicz et al. (1969). The basic ingredient is that, in every loading step, the incremental stress correction vector is computed in terms of plastic parameters corresponding to the incremental radial stress and displacement, starting from the previous step, using (14), (21) for the isotropic case and (46), (47), (49), (54), (55) for the anisotropic case.

In order to solve numerically the problem of a multilayered tube, special care must be given in the interfaces between the individual layers. In this work we approximate the discontinuities between two layers in the radial direction with sharp but continuous and smooth functions. For this reason we choose the sigmoid function (Seto and Nishimura, 2004; Chatzigeorgiou et al., 2007)

$$m(r)=\frac{1}{1/m_1-\frac{1/m_1-1/m_2}{1+e^{-wr}}}, \tag{61}$$

where m_1 and m_2 are the mechanical properties of two neighbor layers and w is a parameter which controls the sharpness of the interface region. This approximation produces continuous stresses and displacements in the r direction, allowing the use of the finite difference method.

We will present the numerical simulation of the isotropic case, the anisotropic case being treated in exactly the same manner. The system of equations (6) and (7), with boundary conditions (8) is discretized with the help of finite differences,

$$-\frac{1}{2\delta r}\dot{\sigma}_{r_{i-1}}+\frac{1-N}{r_i}\dot{\sigma}_{r_i}-\frac{1-N^2}{r_i^2}A_i\dot{u}_i+\frac{1}{2\delta r}\dot{\sigma}_{r_{i+1}}=-\frac{1-N^2}{r_i}A_i\dot{\lambda}_i, \tag{62}$$

$$-\frac{A_i/A_{i-1}}{2\delta r}A_{i-1}\dot{u}_{i-1}-\dot{\sigma}_{r_i}+\frac{N}{r_i}A_i\dot{u}_i+\frac{A_i/A_{i+1}}{2\delta r}A_{i+1}\dot{u}_{i+1}=-(1-N)A_i\dot{\lambda}_i, \tag{63}$$

$i=2,3\ldots,k-2,k-1$. At the end points, the equilibrium equation is written

$$\left(\frac{1-N}{a}-\frac{3}{2\delta r}\right)\dot{\sigma}_{r_1}-\frac{1-N^2}{a^2}A_1\dot{u}_1+\frac{2}{\delta r}\dot{\sigma}_{r_2}-\frac{1}{2\delta r}\dot{\sigma}_{r_3}=-\frac{1-N^2}{a}A_1\dot{\lambda}_1, \tag{64}$$

$$\frac{1}{2\delta r}\dot{\sigma}_{r_{k-2}}-\frac{2}{\delta r}\dot{\sigma}_{r_{k-1}}+\left(\frac{1-N}{b}+\frac{3}{2\delta r}\right)\dot{\sigma}_{r_k}-\frac{1-N^2}{b^2}A_k\dot{u}_k=-\frac{1-N^2}{b}A_k\dot{\lambda}_k. \tag{65}$$

Moreover, the boundary conditions are written as

$$\dot{\sigma}_{r_1}=-\dot{p}_i,\quad \dot{\sigma}_{r_k}=0. \tag{66}$$

From the previous formulation and for computational reasons only we determine at each point $\dot{\sigma}_{r_i}$ and $A_i\dot{u}_i$. For the computation of the plastic strains we follow an iterative method. We consider a pseudo time τ. For small increment of τ the iterative procedure is the following: (a) At time τ we know all the variables. (b) At time $\tau+\Delta\tau$ and at the step s we solve the system of equations (6) and (7), with boundary conditions (8) and we determine ${}^{\tau+\Delta\tau}\dot{\sigma}^s_{r_i}$, ${}^{\tau+\Delta\tau}\dot{\epsilon}^s_{\theta_i}$. (c) For all the points in the elastic region ${}^{\tau+\Delta\tau}\dot{\lambda}^s_i=0$, while for all the points in the plastic region

$${}^{\tau+\Delta\tau}\dot{\lambda}^s_i={}^{\tau+\Delta\tau}\dot{\epsilon}^s_{\theta_i}-\frac{1}{A_i(1+N)}{}^{\tau+\Delta\tau}\dot{\sigma}^s_{r_i}.$$

The increment of stress σ^s_θ is written with the help of (3) and the yield condition (10),

$${}^{\tau+\Delta\tau}\dot{\sigma}^s_{\theta_i}=\begin{cases}N^{\tau+\Delta\tau}\dot{\sigma}^s_{r_i}+(1-N^2)A^{\tau+\Delta\tau}\dot{\epsilon}^s_{\theta_i}, & {}^{\tau+\Delta\tau}\dot{\lambda}^s_i=0,\\ {}^{\tau+\Delta\tau}\dot{\sigma}^s_{r_i}+\left({}^{\tau}\sigma_{r_i}+\sigma_{0_i}-{}^{\tau}\sigma^s_{\theta_i}\right)/\Delta\tau, & {}^{\tau+\Delta\tau}\dot{\lambda}^s_i>0.\end{cases}$$

(d) The total stresses are given by the relations

$${}^{\tau+\Delta\tau}\sigma^s_{r_i}={}^{\tau}\sigma_{r_i}+{}^{\tau+\Delta\tau}\dot{\sigma}^s_{r_i}\Delta\tau,$$
$${}^{\tau+\Delta\tau}\sigma^s_{\theta_i}={}^{\tau}\sigma_{\theta_i}+{}^{\tau+\Delta\tau}\dot{\sigma}^s_{\theta_i}\Delta\tau,$$
$${}^{\tau+\Delta\tau}\sigma^s_{z_i}=\nu\left({}^{\tau+\Delta\tau}\sigma^s_{r_i}+{}^{\tau+\Delta\tau}\sigma^s_{\theta_i}\right).$$

If the change in the sum of $\sigma_i=(\sigma^2_{ri}+\sigma^2_{\theta i}+\sigma^2_{zi})^{1/2}$ between steps $s-1$ and s at all the points is greater than a specific limit, then we return to step (b). Otherwise all the variables at time $\tau+\Delta\tau$ are determined and we proceed to the next time increment.

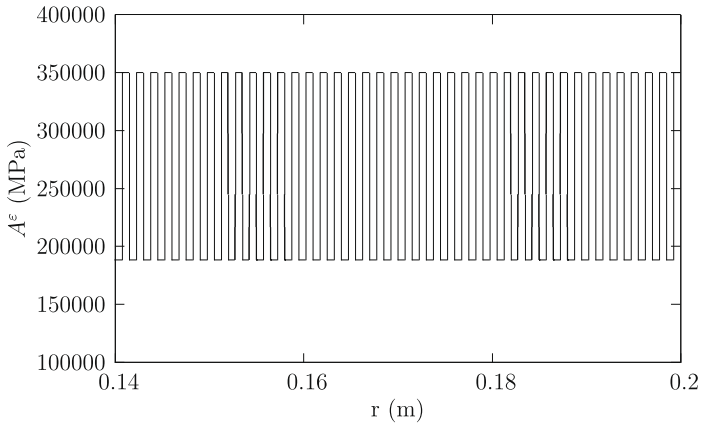

Fig. 2. Periodic material: variation of the elastic coefficient with respect to the radius.

The numerical solution was obtained with the help of a FORTRAN code. The system of equations (6)–(8) was solved with the use of special routines (Anderson et al., 1999). The numerical method proposed here was tested with the use of some examples from the literature. Solving the tube of homogeneous material (Chen and Han, 1988, page 203) or functionally graded material (Eraslan and Akis, 2005), the numerical method presents an error in the failure load less than 0.1% from the theoretical values. In the example of Chen and Han (1988), the incompressible material was simulated with $\nu = 0.499$.

For the homogenized material, Eqs. (62)–(65) are written as

$$-\frac{1}{2\delta r}\dot{\sigma}^h_{r_{i-1}}+\frac{1-N}{r_i}\dot{\sigma}^h_{r_i}-\frac{1-N^2}{r_i^2}\langle A^\varepsilon\rangle\langle 1/A^\varepsilon\rangle\frac{\dot{u}^h_i}{\langle 1/A^\varepsilon\rangle}+\frac{1}{2\delta r}\dot{\sigma}^h_{r_{i+1}}=-\frac{1-N^2}{r_i}\dot{\Lambda}^h_i, \tag{67}$$

$$-\frac{1}{2\delta r}\frac{\dot{u}^h_{i-1}}{\langle 1/A^\varepsilon\rangle}-\dot{\sigma}^h_{r_i}+\frac{N}{r_i}\frac{\dot{u}^h_i}{\langle 1/A^\varepsilon\rangle}+\frac{1}{2\delta r}\frac{\dot{u}^h_{i+1}}{\langle 1/A^\varepsilon\rangle}=-\frac{1-N}{\langle 1/A^\varepsilon\rangle}\dot{\lambda}^h_i, \tag{68}$$

$i = 2,3\ldots,k-2,k-1$. At the end points, equilibrium equation is written

$$\left(\frac{1-N}{a}-\frac{3}{2\delta r}\right)\dot{\sigma}^h_{r_1}-\frac{1-N^2}{a^2}\langle A^\varepsilon\rangle\langle 1/A^\varepsilon\rangle\frac{\dot{u}^h_1}{\langle 1/A^\varepsilon\rangle}+\frac{2}{\delta r}\dot{\sigma}^h_{r_2}-\frac{1}{2\delta r}\dot{\sigma}^h_{r_3}=-\frac{1-N^2}{a}\dot{\Lambda}^h_1, \tag{69}$$

$$\frac{1}{2\delta r}\dot{\sigma}^h_{r_{k-2}}-\frac{2}{\delta r}\dot{\sigma}^h_{r_{k-1}}+\left(\frac{1-N}{b}+\frac{3}{2\delta r}\right)\dot{\sigma}^h_{r_k}-\frac{1-N^2}{b^2}\langle A^\varepsilon\rangle\langle 1/A^\varepsilon\rangle\frac{\dot{u}^h_k}{\langle 1/A^\varepsilon\rangle}=-\frac{1-N^2}{b}\dot{\Lambda}^h_k. \tag{70}$$

From the previous formulation we determine at each point $\dot{\sigma}^h_{r_i}$ and $\frac{\dot{u}^h_i}{\langle 1/A^\varepsilon\rangle}$.

The computational process is similar with the process of the periodic material. However, in step (c) we compute two plastic work-dependent multipliers, $\dot{\lambda}^h_i$ and $\dot{\Lambda}^h_i$ from Eq. (21).

5. Numerical examples

We first consider a hollow cylinder consisting of 80 thin periodic layers made of two isotropic materials (Fig. 1). Our intention is to investigate the character of the non-homogeneous material, when the parameter ε tends to zero, which is interpreted as infinite number of layers. In this example, 80 layers where sufficient to reach the limited response of the actual material. The mechanical parameter A^ε and the yield stress σ^ε_0 of the cylinder varies periodically, as it is shown in Figs. 2 and 3, with average values of the Young modulus and the yield stress $\langle\sigma^\varepsilon_0\rangle = 200$ MPa and $\langle E_0\rangle = 200$ GPa, respectively. The Poisson ratio is equal to 0.3. In the numerical simulation, $A^\varepsilon(r)$ and σ_0 are approximated by sigmoid functions, where the parameter w has been chosen to be equal to 1.E7. The radial stress is equal to $-p_i$ at the inner surface and zero at the outer surface. The pressure p_i increases progressively, until the failure of the tube. The inner and outer radii are $a = 0.14$ m and $b = 0.2$ m, respectively. The numerical solution of the problem is based on the procedure described in the previous section. In the analysis, 10001 equidistant nodes are used. The elastic stiffness matrices of the two distinct layers are (the units are in GPa)

$$\begin{bmatrix} 188.46 & 80.77 \\ 80.77 & 188.46 \\ 80.77 & 80.77 \end{bmatrix}, \begin{bmatrix} 350 & 150 \\ 150 & 350 \\ 150 & 150 \end{bmatrix}.$$

In Fig. 4, we show a non-dimensional stress–strain curve, based on Chen and Han, 1988, p. 203. The failure occurs at $p_i = 71.23$ MPa. Following Eraslan and Akis, 2005, we present in Fig. 5 non-dimensional diagrams at a pressure level $p_i = 66.542$ MPa, where $\bar{r} = r/b$, $\bar{u}^\varepsilon = u^\varepsilon\langle E_0\rangle/\left(b\langle\sigma^\varepsilon_0\rangle\right)$, $\bar{\sigma}^\varepsilon_j = \sigma^\varepsilon_j/\langle\sigma^\varepsilon_0\rangle$, $\bar{\epsilon}^{p\varepsilon}_j = \epsilon^{p\varepsilon}_j\langle E_0\rangle/\langle\sigma^\varepsilon_0\rangle$, $j = r, \theta, z$ and $\dot{\bar{\lambda}}^\varepsilon = 100\dot{\lambda}^\varepsilon\langle E_0\rangle/\langle\sigma^\varepsilon_0\rangle$. Regarding the variation of the plastic multiplier $\dot{\bar{\lambda}}^\varepsilon$ we observe that there are three zones in the tube: one totally plastic from the inner radius to $r = 0.16925$ m (end of the 39th layer), one with successive elastic and plastic regions from $r = 0.16925$ m to $r = 0.172244$ m (end of the 43rd layer) and one totally elastic from $r = 0.172244$ m to the outer radius. The variation of the incremental stress with respect to radius for two differ-

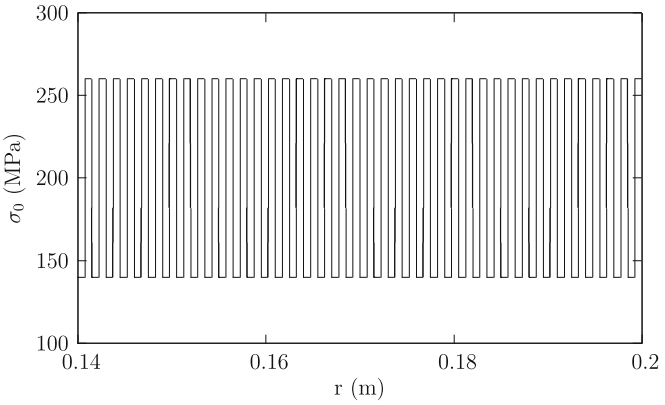

Fig. 3. Periodic material: variation of the yield stress with respect to the radius.

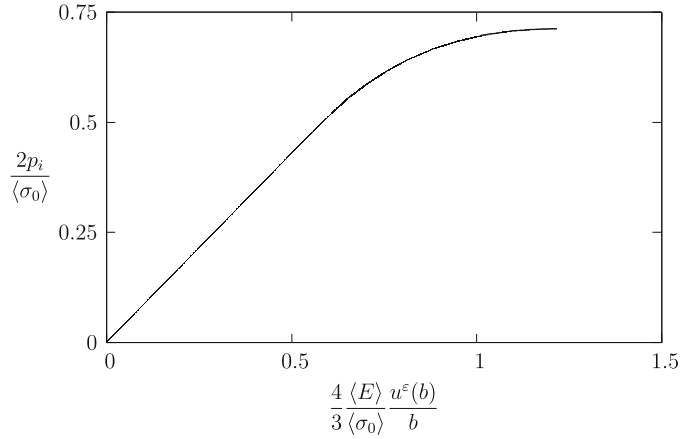

Fig. 4. Periodic material: the relation between internal pressure and displacement.

ent pressure levels is shown in Fig. 6. Finally, we present the stress, displacement and strain variation with respect to radius at the failure in Fig. 7.

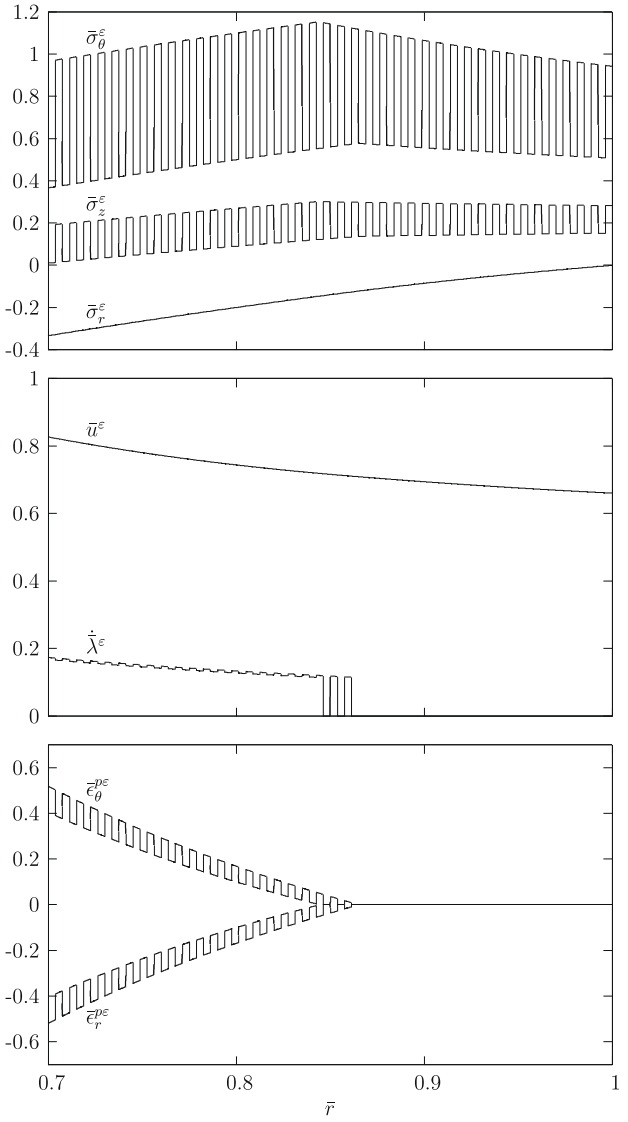

Fig. 5. Periodic material: variation of stresses, displacement and strains with respect to the radius for $p_i = 66.542$ MPa.

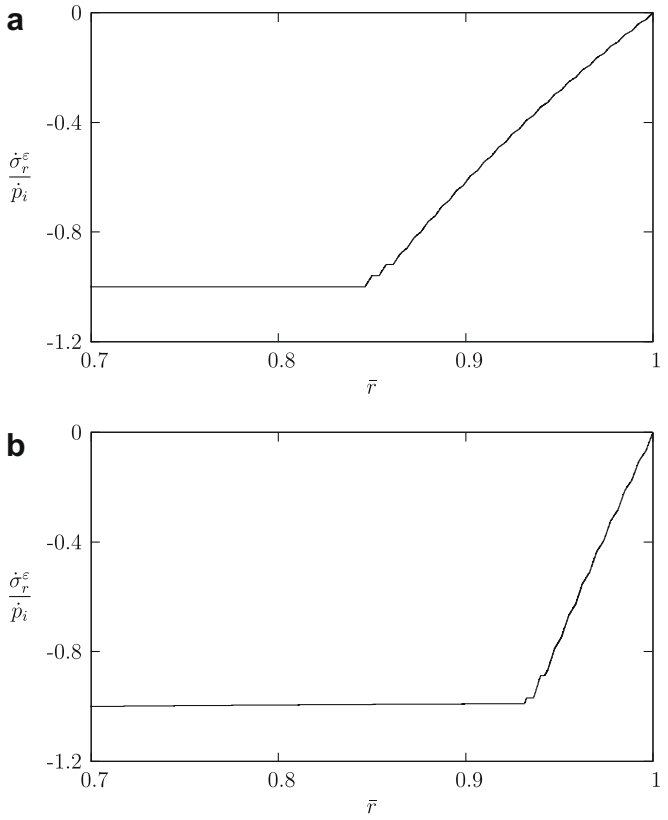

Fig. 6. Periodic material: variation of incremental stress with respect to the radius for (a) $p_i = 66.542$ MPa and (b) $p_i = 70.35$ MPa.

Next, we proceed to the homogenized material. The computational procedure was described in the previous section. The elastic stiffness matrix of the effective medium is (the units are in GPa)

$$\begin{bmatrix} 245 & 105 \\ 105 & 264.78 \\ 105 & 110.93 \end{bmatrix}.$$

Additionally the two plastic coefficients are given by the expressions

$$\dot\lambda^h = \frac{\dot u^h}{r} - 2.857\times 10^{-6}\dot\sigma^h_r, \quad \dot\Lambda^h = 269231\frac{\dot u^h}{r} - 0.7\dot\sigma^h_r.$$

In Fig. 8 we compare the stress–strain diagram between the non-homogeneous and the homogenized material. The two curves seem to practically coincide. The homogenized material fails at inner pressure equal to 71.32 MPa, which differs from the failure pressure of the non-homogeneous material by 0.126%. At a pressure $p_i = 66.542$ MPa we present the variation of non-dimensional stresses, plastic strains and displacements with respect to radius at Fig. 9, where the plastic parameters are $\dot{\bar\lambda}^h$ and $\dot{\bar\Lambda}^h = 100\dot\Lambda^h/\langle\sigma^\varepsilon_0\rangle$. Two zones exist: one totally plastic from the inner radius to $r = 0.16994$ m and one totally elastic from $r = 0.16994$ m (end of the 40th layer of the periodic material) to the outer radius. The different number of elastic–plastic zones in the solution of inhomogeneous and homogenized problems is due to the oscillations of radial and angular plastic strains $\epsilon^{p\varepsilon}_r, \epsilon^{p\varepsilon}_\theta$, approaching 0. We note that the absence of the intermediate zone causes increase of the elastic zone in the homogenized material. The length of the totally plastic zone of the homogenized material differs from the corresponding length of the non-homogeneous material by 0.47%. The variation of the incremental stress with respect to radius (for the same pressure levels with these of the non-homogeneous material depicted in Fig. 6)

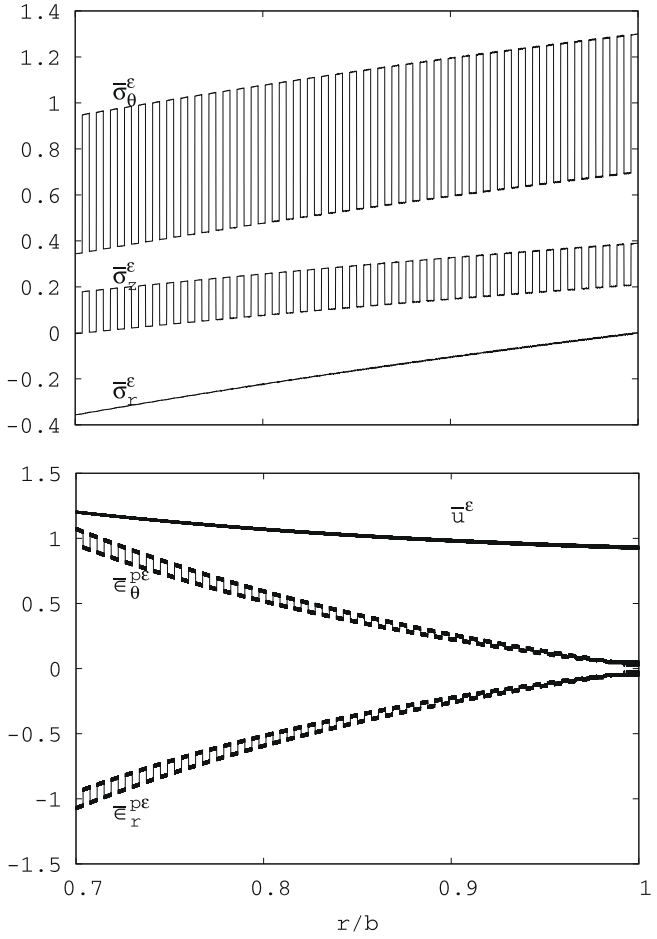

Fig. 7. Periodic material: Variation of stresses, displacement and strains with respect to the radius at failure.

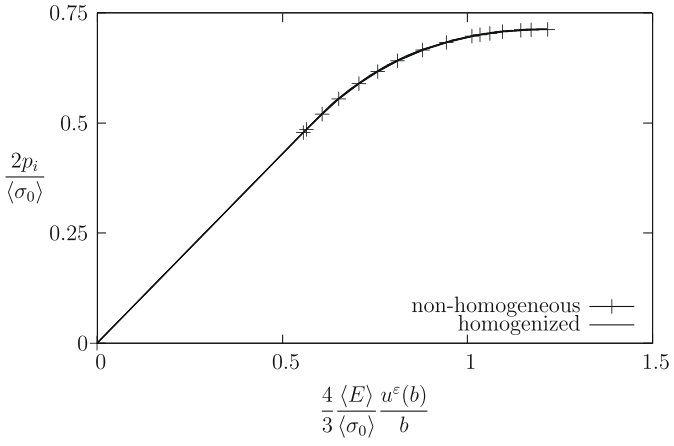

Fig. 8. The relation between internal pressure and displacement for the non-homogeneous and for the homogenized material.

is shown in Fig. 10. Finally, in Fig. 11, we present the stress, displacement and strain variation with respect to radius at the failure.

In the next example, we consider a hollow cylinder consisting of 80 thin periodic layers made of two orthotropic materials. The first material is graphite/epoxy laminae, where the elastic mechanical characteristics are based on Tarn and Wang (2001). The second material is produced by the first one by 30% increase of its mechanical properties. The stiffness matrices of the two materials are

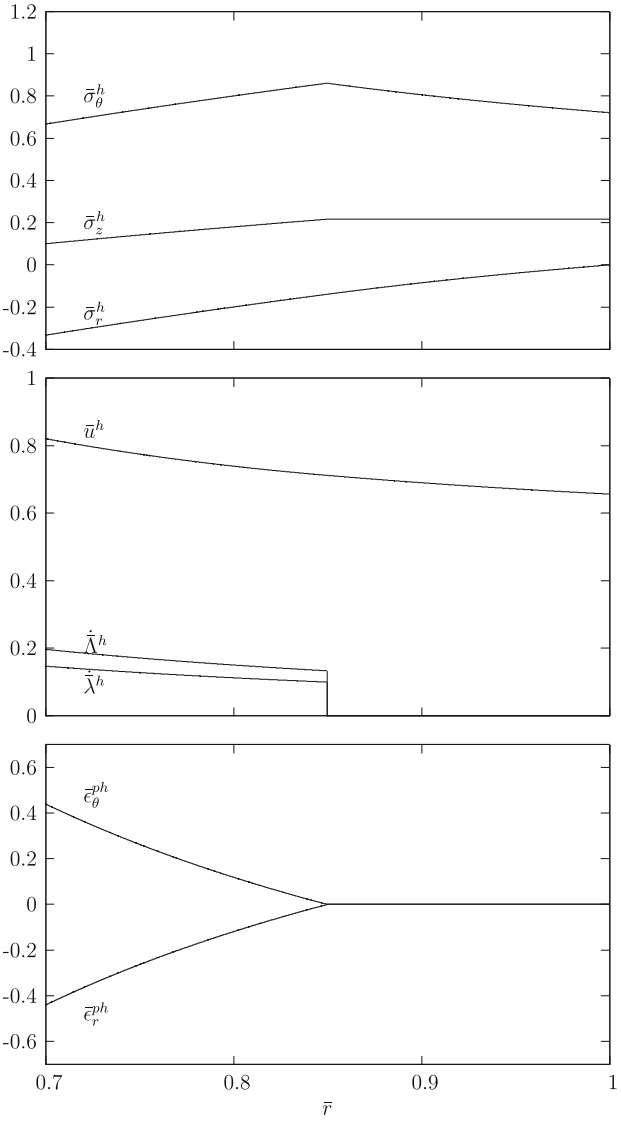

Fig. 9. Homogenized material: variation of stresses, displacement and strains with respect to the radius for $p_i = 66.542$ MPa.

$$\begin{bmatrix} 139.638 & 3.9 \\ 3.9 & 15.278 \\ 3.9 & 3.294 \end{bmatrix}, \begin{bmatrix} 181.53 & 5.07 \\ 5.07 & 19.861 \\ 5.07 & 4.28 \end{bmatrix},$$

where the units are in GPa. The two layers are assumed to have the same yield stress, equal to 200 MPa. The geometry and the meshing of the tube is exactly the same with the one of the previous example.

Even though the elastic constants of the layers do not satisfy the inequalities (39), in the analysis performed, there is no point or pressure level where the stresses violated the basic inequality (9) (see for instance the stress-radius curves in Fig. 13). This allows us to use the results for the effective properties obtained at Section 3.

In Fig. 12 we observe that the multilayered tube fails at internal pressure equal to 71.3. The homogenized material's response is very close to that of the non-homogeneous. Fig. 13 shows again three different zones of the tube, starting from the inner radius: one totally plastic until the end of the 8th layer, one with elastic and plastic regions until the end of the 31st layer and on completely elastic until the outer surface of the tube. The tube with

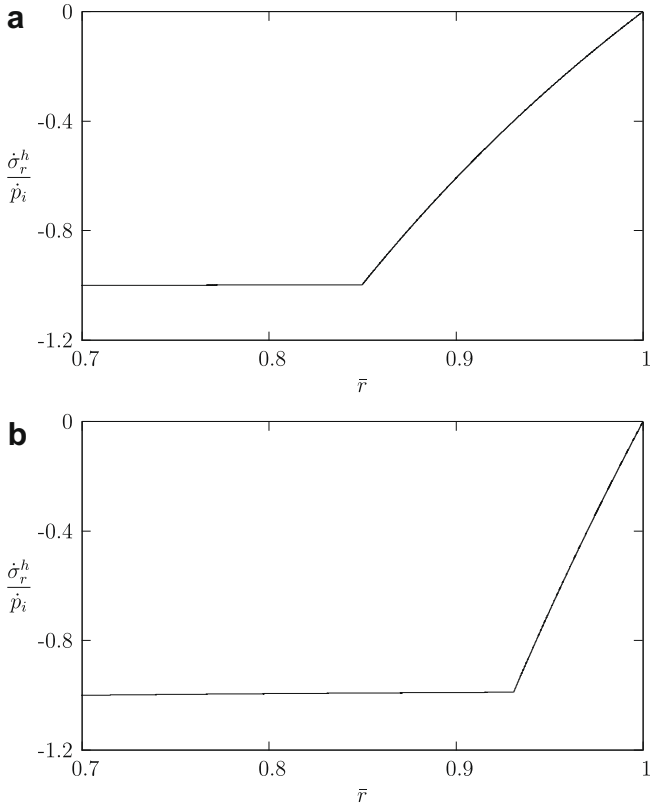

Fig. 10. Homogenized material: variation of incremental stress with respect to the radius for (a) $p_i = 66.542$ MPa and (b) $p_i = 70.35$ MPa.

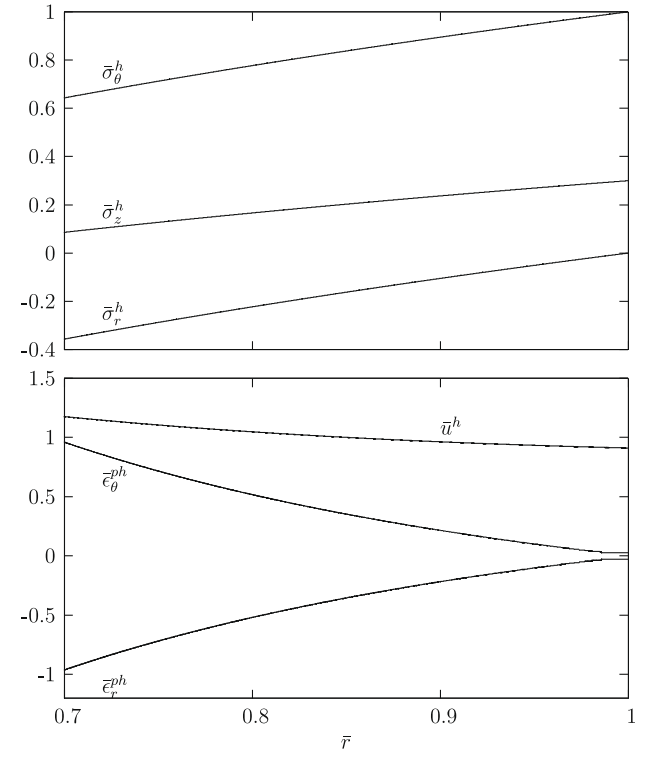

Fig. 11. Homogenized material: variation of stresses, displacement and strains with respect to the radius at failure.

the homogenized material has two zones (Fig. 14), one totally plastic until the middle of the 18th layer of the multilayered tube,

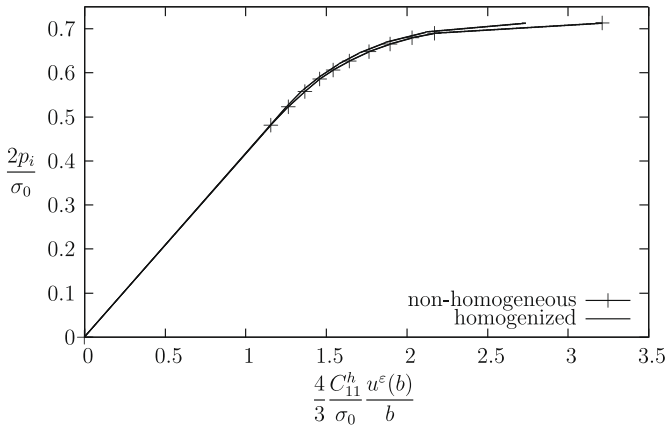

Fig. 12. Relation between internal pressure and displacement for the non-homogeneous orthotropic material and the homogenized.

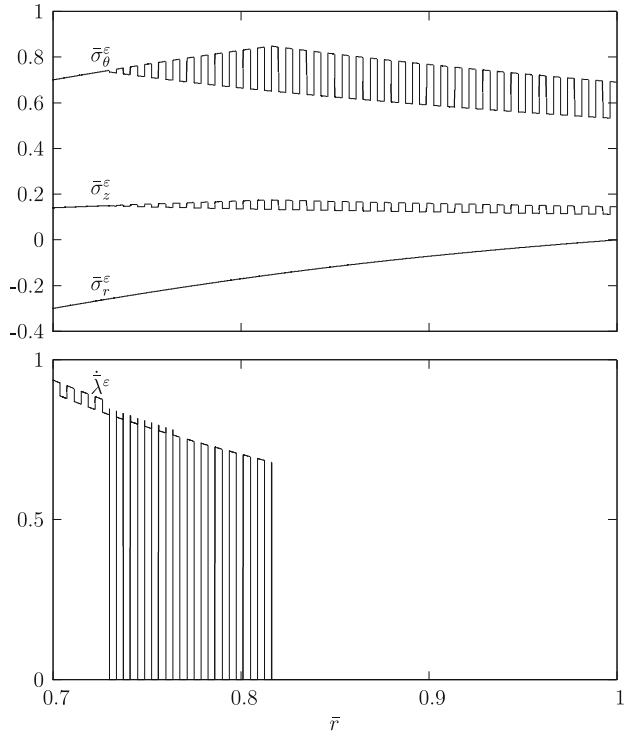

Fig. 13. Periodic orthotropic layers: variation of stresses and plastic multiplier with respect to the radius at $p_i = 60$ MPa.

and one elastic until the external radius. The plastic parameters in Figs. 13 and 14 are normalized according to the relations $\dot{\bar{\lambda}}^\varepsilon = 100 C_{11}^h \dot{\lambda}^\varepsilon/\sigma_0, \dot{\bar{\lambda}}^h = 100 C_{11}^h \dot{\lambda}^h/\sigma_0, \dot{\bar{\Lambda}}_1^h = 100 C_{11}^h \dot{\Lambda}_1^h/\sigma_0, \dot{\bar{\Lambda}}_2^h = 100 \dot{\Lambda}_2^h/\sigma_0, \dot{\bar{\Lambda}}_3^h = 100 \dot{\Lambda}_3^h/\sigma_0$.

6. Conclusion

In this work, the homogenization of a periodic elastic–perfectly plastic pressurized tube made of very dissimilar materials is presented. The problem is stable by homogenization, in the sense that the equations of the heterogeneous and of the effective medium have the same form, provided that the incremental stress–strain matrix equation is expressed in terms of the elastic stiffness matrix and the incremental stress correction vector. This formulation excludes the production of the rate of elastic and plastic effective

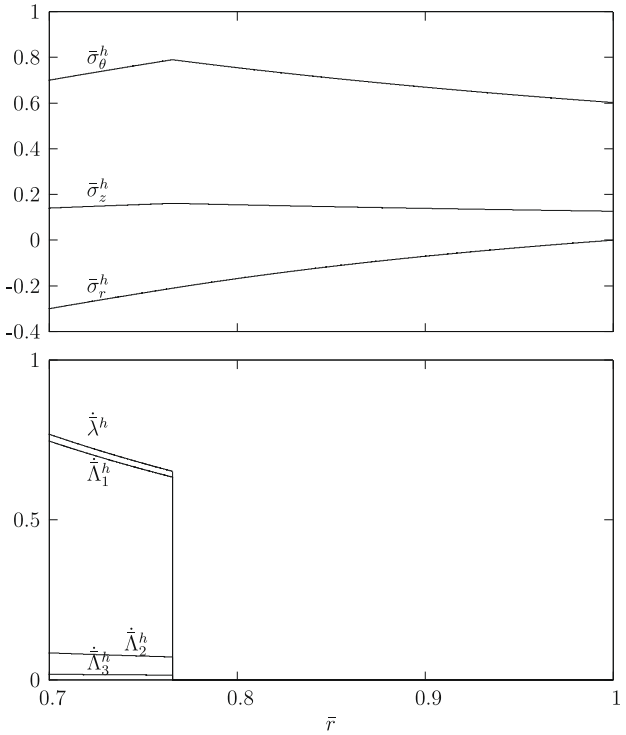

Fig. 14. Homogenized material: variation of stresses and plastic multipliers with respect to the radius at $p_i = 60$ MPa.

strain by ensemble averaging the corresponding heterogeneous quantities. This result can be compared with the results of other researchers, concerning the effective strain-rate. However, contrarily to Hill's approach, which is based on the use of tangent modulus, the incremental stress correction vector-based approach in the present paper leads to solving the effective material independently of the corresponding heterogeneous medium, since effective coefficients are given by explicit formulas. In the present work, we quantify the elastic and plastic behavior of the effective medium and explain the homogenization-induced anisotropies for the isotropic materials. In the case of orthotropic materials, the effective incremental stress correction vector contains three independent plastic work-dependent parameters.

Appendix A

The first and the third equations (16) for a cylindrically anisotropic material take the form (Chatzigeorgiou et al., 2008)

$$\frac{d\sigma_r^\varepsilon}{dr}+\frac{1-C_{12}^\varepsilon/C_{11}^\varepsilon}{r}\sigma_r^\varepsilon=\frac{C_{11}^\varepsilon C_{22}^\varepsilon-\left(C_{12}^\varepsilon\right)^2}{r^2C_{11}^\varepsilon}u^\varepsilon,\quad \frac{du^\varepsilon}{dr}+\frac{C_{12}^\varepsilon}{rC_{11}^\varepsilon}u^\varepsilon=\frac{\sigma_r^\varepsilon}{C_{11}^\varepsilon}, \tag{A-1}$$

where C_{ij}^ε the material constants, bounded from above and from below. We put

$$e^{\int_a^r\frac{1-C_{12}^\varepsilon(\xi)/C_{11}^\varepsilon(\xi)}{\xi}d\xi}=\phi^\varepsilon(r),\quad e^{\int_a^r\frac{C_{12}^\varepsilon(\xi)}{\xi C_{11}^\varepsilon(\xi)}d\xi}=\chi^\varepsilon(r),$$
$$\frac{C_{11}^\varepsilon(r)C_{22}^\varepsilon(r)-\left(C_{12}^\varepsilon(r)\right)^2}{r^2C_{11}^\varepsilon(r)}=\psi^\varepsilon(r)>0. \tag{A-2}$$

Properties of functions ϕ^ε, χ^ε and ψ^ε, such as the positiveness of ψ^ε, are due to (40). Then, by using the boundary condition $\sigma_r^\varepsilon(a)=-p_i$, we obtain from equations (A-1)

$$\sigma_r^\varepsilon(r)=\frac{1}{\phi^\varepsilon(r)}\left(-p_i+\int_a^r\phi^\varepsilon(\xi)\psi^\varepsilon(\xi)u^\varepsilon(\xi)d\xi\right), \tag{A- 3}$$

$$u^\varepsilon(r)=\frac{1}{\chi^\varepsilon(r)}\left(u^\varepsilon(a)+\int_a^r\chi^\varepsilon(\xi)\frac{\sigma_r^\varepsilon(\xi)}{C_{11}^\varepsilon(\xi)}d\xi\right), \tag{A-4}$$

where $u^\varepsilon(a)$ is the unknown value of u^ε at $r=a$. Combining equations (A-3) and (A-4) gives

$$\sigma_r^\varepsilon(r)=\frac{1}{\phi^\varepsilon(r)}\left[-p_i+u^\varepsilon(a)\int_a^r\zeta^\varepsilon(\xi)d\xi+\int_a^r\zeta^\varepsilon(\xi)\left(\int_a^\xi\chi^\varepsilon(s)\frac{\sigma_r^\varepsilon(s)}{C_{11}^\varepsilon(s)}ds\right)d\xi\right]. \tag{A-5}$$

where

$$\zeta^\varepsilon(r)=\phi^\varepsilon(r)\psi^\varepsilon(r)/\chi^\varepsilon(r)>0. \tag{A-6}$$

Based on the above equations, we examine all possible combinations (Chatzigeorgiou et al., 2008) of $sign(u^\varepsilon(a))$ and behavior of u^ε and σ^ε and prove that $u^\varepsilon(r)>0$ monotone decreasing function and $\sigma_r^\varepsilon(r)\leqslant 0$ monotone increasing function for every $a\leqslant r\leqslant b$. Using (A-3) and (A-4) and the properties of ϕ^ε and χ^ε leads to the boundedness of the L^∞-norms of $u^\varepsilon(r)$ and $\sigma_r^\varepsilon(r)$ independently of ε. Then, by using (A-1) we show that the L^∞-norms of $\frac{du^\varepsilon}{dr}$ and $\frac{d\sigma_r^\varepsilon}{dr}$ too are bounded independently of ε. Then, there exist a subsequence $\sigma_r^{\varepsilon'}$, still denoted by σ_r^ε, and a σ_r^h, and a subsequence $u^{\varepsilon'}$, still denoted by u^ε, and a u^h such that

$$\sigma_r^\varepsilon\to\sigma_r^h\quad\text{in } C(a,b), \tag{A- 7}$$

$$u^\varepsilon\to u^h\quad\text{in } C(a,b), \tag{A-8}$$

and we can pass to the limit in (A-1). The system of the second and the forth equations (16) may be treated in a similar way, using the continuity conditions for $u^\varepsilon(r)$ and $\sigma_r^\varepsilon(r)$ at all common points of elastic and plastic regions.

Appendix B

From Appendix A we conclude that there exists only the case $u^\varepsilon(r)>0$ and $\sigma_r^\varepsilon(r)\leqslant 0$, where $\sigma_r^\varepsilon(r)$ is a monotone increasing function from $-p_i$ to zero. Then, from the equilibrium equation

$$\sigma_\theta^\varepsilon(r)>\sigma_r^\varepsilon(r). \tag{B-1}$$

In the case of an isotropic material, the stresses in the elastic region are written as

$$\sigma_\theta^\varepsilon(r)=N\sigma_r^\varepsilon(r)+\frac{1-N^2}{r}Au^\varepsilon(r),\sigma_z^\varepsilon(r)=\nu\left(\sigma_r^\varepsilon(r)+\sigma_\theta^\varepsilon(r)\right). \tag{B-2}$$

For $\nu<0.5$ ($N<1$), $u^\varepsilon(r)>0$ leads to $\sigma_\theta^\varepsilon(r)>N\sigma_r^\varepsilon(r)$, or, due to (4) and (B-2)$_2$,

$$\sigma_\theta^\varepsilon(r)>\sigma_z^\varepsilon(r). \tag{B-3}$$

Finally, $\sigma_r^\varepsilon(r)\leqslant 0$ and $N<1$ implies that $N\sigma_r^\varepsilon(r)\geqslant\sigma_r^\varepsilon(r)$, or $2\nu\sigma_r^\varepsilon(r)\geqslant\sigma_r^\varepsilon(r)$. (B-1) and (B-2)$_2$ lead to $\sigma_z^\varepsilon(r)>2\nu\sigma_r^\varepsilon(r)$, so

$$\sigma_z^\varepsilon(r)>\sigma_r^\varepsilon(r). \tag{B-4}$$

References

Anderson, E., Bai, Z., Bischof, C., Blackford, S., Demmel, J., Dongarra, J., Croz, J.D., Greenbaum, A., Hammarling, S., McKenney, A., Sorensen, D., 1999. LAPACK Users' Guide, third ed. SIAM, Philadelphia.

Babuska, I., 1976a. Homogenization and its application: mathematical and computational problems. In: Numerical Solution of Partial Differential Equations-III (SYNSPADE 1975). Academic Press, New York, pp. 89–116.

Babuska, I., 1976b. Homogenization approach in engineering. In: Computing Methods in Applied Sciences and Engineering (Second International Symposium, Versailles, 1975), Part 1, Lecture Notes in Economics and Mathematical Systems, vol. 134. Springer, Berlin, pp. 137–153.

Bakhalov, N., Panasenko, G., 1989. Homogenisation: Averaging Processes in Periodic Media. Mathematical Problems in the Mechanics of Composite Materials. Kluwer Academic Publishers, Dordrecht.

Batra, R., Adulla, C., 1995. Effect of prior quasi-static loading on the initiation and growth of dynamic adiabatic shear bands. Archives of Mechanics 47 (3), 485–498.

Batra, R.C., Lear, M.H., 2005. Adiabatic shear banding in plane strain tensile deformations of 11 thermoviscoplastic materials with finite thermal wave speed. International Journal of Plasticity 21, 1521–1545.

Batra, R.C., Love, B.M., 2004. Adiabatic shear bands in functionally graded materials. Journal of Thermal Stresses 27, 1101–1123.

Batra, R.C., Rattazi, D., 1997. Adiabatic shear banding in a thick-walled steel tube. Computational Mechanics 20, 412–426.

Bensoussan, A., Lions, J.-L., Papanicolaou, G., 1978. Asymptotic Methods for Periodic Structures. North-Holland, Amsterdam.

Berman, I., Hodge, P.G., 1959. A general theory of piecewise linear plasticity for initially anisotropic materials. Archiwum Mechaniki Stosowanej 11, 513–540.

Boussaa, D., 2006. Optimizing the composition profile of a functionally graded interlayer using a direct transcription method. Computational Mechanics 39 (3), 59–71.

Burns, T., Davies, M.A., 2002. On repeated adiabatic shear band formation during high-speed machining. International Journal of Plasticity 18, 487–506.

Charalambakis, N., Murat, F., 2007. Stability by homogenization of thermoviscoplastic problems. Publications du laboratoire Jacques-Louis Lions, R07013, p. 73, electronic version available at the URL: <http://www.ann.jussieu.fr/>.

Chatterjee, D., 1970. Some problems of plane strain in a non-homogeneous isotropic cylinder. Pure and Applied Geophysics 82 (1), 34–40.

Chatzigeorgiou, G., Charalambakis, N., Kalpakides, V., 2007. Biaxial loading of continuously graded thermoviscoplastic materials. Computational Mechanics 39 (4), 335–355.

Chatzigeorgiou, G., Charalambakis, N., Murat, F., 2008. Homogenization problems of a hollow cylinder made of elastic materials with discontinuous properties. International Journal of Solids and Structures 45, 5165–5180.

Chen, W.F., Han, D.J., 1988. Plasticity for Structural Engineers. Springer, Berlin.

Chen, T., Chung, C.-T., Lin, W.-L., 2000. A revisit of a cylindrically anisotropic tube subjected to pressuring, shearing, torsion, extension and a uniform temperature change. International Journal of Solids and Structures 37, 5143–5159.

Chen, L., Urquhart, E., Pindera, M.-J., 2005. Microstructural effects in multilayers with large moduli contrast loaded by flat punch. AIAA Journal 43 (5), 962–973.

Drago, A., Pindera, M.-J., 2007. Micro-macromechanical analysis of heterogeneous materials: macroscopically homogeneous vs periodic microstructures. Composites Science and Technology 67, 1243–1263.

Eraslan, A.N., Akis, T., 2005. Elastoplastic response of a long functionally graded tube subjected to internal pressure. Turkish Journal of Engineering and Environmental Sciences 29, 361–368.

Geymonat, G., Krasucki, F., Marigo, J.-J., 1987a. On the commutativity of limiting processes in the asymptotic theory of composite rods. Comptes Rendus de l' Académie de Sciences de Paris, Série II, Mécanique, Physique, Chimie, Sciences de l' Univers, Sciences de la Terre 305 (4), 225–228.

Geymonat, G., Krasucki, F., Marigo, J.-J., 1987b. Stress distribution in anisotropic elastic composite beams. Recherches de Mathematiques Appliquees 4, 118–133.

Hill, R., 1965. Continuum micro-mechanics of elastoplastic polycrystals. Journal of the Mechanics and Physics of Solids 13, 89–101.

Horgan, C., Chan, A., 1999a. The pressurized hollow cylinder or disk problem for functionally graded isotropic linearly elastic materials. Journal of Elasticity 55 (1), 43–59.

Horgan, C., Chan, A., 1999b. The stress response of functionally graded isotropic linearly elastic rotating disks. Journal of Elasticity 55 (1), 219–230.

Hosseini Kordkheili, S., Naghdabadi, R., 2007. Thermoelastic analysis of a functionally graded rotating disk. Composite Structures 79, 508–516.

Khan, A.S., Huang, S., 1995. Continuum Theory of Plasticity. Wiley–Interscience, New York.

Khatam, H., Pindera, M.-J., 2009. Parametric finite-volume micromechanics of periodic materials with elastoplastic phases. International Journal of Plasticity 25 (7), 1386–1411.

Krishnaswamy, S., Beatty, M., 2001. Damage induced stress-softening in the torsion, extension and inflation of a cylindrical tube. Quarterly Journal of Mechanics and Applied Mathematics 54 (2), 295–327.

Lemaitre, J., 2001. Handbook of Materials Behavior Models, vol. 1. Academic Press, New York.

Mukhopadhyay, J., 1982. Effect of non-homogeneity on yield stress in a thick-walled cylindrical tube under pressure. Letters in Applied Engineering Sciences 20 (8), 963–968.

Murat, F., 1977. H-convergence. Séminaire d'analyse fonctionnelle et numérique de l'Université d'Alger.

Qu, J., Cherkaoui, M., 2006. Fundamentals of Micromechanics of Solids. Wiley, New York.

Ruhi, M., Angoshtari, A., Naghdabadi, R., 2005. Thermoelastic analysis of thick-walled finite-length cylinders of functionally graded materials. Journal of Thermal Stresses 28, 391–408.

Sanchez-Palencia, E., 1978. Non-homogeneous Media and Vibration Theory. Lecture Notes in Physics 127. Springer, Berlin.

Seto, T., Nishimura, T., 2004. Study of two-dimensional elasticity on FGM. In: Proceedings of 21st International Congress of Theoretical and Applied Mechanics, Warsaw.

Tarn, J.-Q., 2002a. Exact solutions of a piezoelectric circular tube or bar under extension, torsion, pressuring, shearing, uniform electric loading and temperature change. Proceedings of the Royal Society of London 458, 2349–2367.

Tarn, J.-Q., 2002b. A state space formalism for anisotropic elasticity. Part II: Cylindrical anisotropy. International Journal of Solids and Structures 39, 5157–5172.

Tarn, J.-Q., Wang, Y.-M., 2001. Laminated composite tubes under extension, torsion, bending, shearing and pressuring: a state space approach. International Journal of Solids and Structures 38, 9053–9075.

Tartar, L., 1977. Homogéneisation et compacité par compensation. Cours Peccot, Collège de France.

Zienkiewicz, O., Valliapan, S., King, I., 1969. Elastoplastic solutions of engineering problems. "Initial stress" f.e.m. International Journal for Numerical Methods in Engineering 1, 75–100.